

Preliminary Drying of Oil Palm Fronds Using Concentrated Solar Thermal Power

By

Farid Fawzy Fathy Taha Ellakany

Dissertation submitted in partial fulfillment of

the requirements for the

Bachelor of Engineering (Hons)

(Mechanical Engineering)

SEPTEMBER 2011

Universiti Teknologi PETRONAS
Bandar Seri Iskandar
31750 Tronoh
Perak Darul Ridzuan

CERTIFICATION OF APPROVAL

Preliminary Drying of Oil Palm Fronds Using Concentrated Solar Thermal Power

By

Farid Fawzy Fathy Taha Ellakany

A project dissertation submitted to the
Mechanical Engineering Programme
Universiti Teknologi PETRONAS
in partial fulfillment of the requirement for the
BACHELOR OF ENGINEERING (Hons)
(MECHANICAL ENGINEERING)

Approved by,

(Ir. Dr. Shaharin Anwar Sulaiman)

UNIVERSITI TEKNOLOGI PETRONAS

TRONOH, PERAK

SEPTEMBER 2011

CERTIFICATION OF ORIGINALITY

This is to certify that I am responsible for the work submitted in this project, that the original work is my own except as specified in the references and acknowledgements, and that the original work contained herein have not been undertaken or done by unspecified sources or persons.

FARID FAWZY FATHY TAHA

ABSTRACT

Biomass is an important renewable energy source. Malaysia has a great potential for biomass stock and especially oil palm wastes. The fact that oil palm fronds contain high moisture content makes it unsuitable to be used directly as a biomass fuel, neither for direct combustion nor gasification. In addition, conventional and costly drying methods make the fronds a non-attractive fuel. The objective of this paper is to find a cheap, sustainable and efficient way of drying oil palm fronds. A new design is proposed that utilizes concentrated solar thermal energy for drying the biomass. A solar dryer rig has been designed and fabricated. The system's target is to maximize the thermal energy received into the system and to minimize energy loss out of it. The rig consists of three main components. A 49 inch Fresnel lens with a concentration ratio of 8 is used for concentrating the solar energy onto a receiver. The second component is the lens holder that provides the needed elevation for the lens according to the required temperature inside the drying chamber, having the maximum temperature at an elevation equals to the focal length. The third component is the drying chamber. It consists of a sheet of aluminum painted in black and a glazing made of 12 mm acrylic sheets. The aluminum sheet which acts as the receiver is designed to receive solar radiation at different times of the day; thus eliminating the need for a sun tracking system. The glazing is used for trapping the heat energy inside the drying chamber, and minimizing conduction of the heat to the surrounding environment. The chamber contains perforations in order to provide air flow inside the chamber; for a faster removal of humidity. Experiments have been performed on samples of oil palm fronds at a drying temperature not exceeding 110°C; in order not to affect the organic material of the biomass. Results have been compared with another experiment that used an electric oven for drying at the same temperature. Using the proposed system, the samples were completely dried in 6.5 hours with an average efficiency of 55.4%, compared to 10.5 hours when using the electric oven. The proposed system achieved an average drying rate of 4.75 g/hr compared to an average drying rate of 2.83 g/hr using the electric oven. These results were achieved since relative humidity value inside the drying chamber was lower compared to that inside the oven. One drawback of the system is its heavy dependence

on the weather. Cloudy conditions affect the results severely. It is recommended to combine another source of heating to the current one. By converting the proposed system into a hybrid one the problem of inconsistent solar radiation can be reduced.

TABLE OF CONTENTS

CERTIFICATION OF APPROVAL	ii
CERTIFICATION OF ORIGINALITY	iii
ABSTRACT	iv
TABLE OF CONTENTS	vi
LIST OF FIGURES	viii
LIST OF TABLES	ix
CHAPTER 1:	INTRODUCTION	1
	1.1 Background of Study	1
	1.2 Problem Statement	3
	1.3 Objective	3
	1.4 Scope of Supply	3
CHAPTER 2:	LITERATURE REVIEW	5
	2.1 Refracting Concentrators	5
	2.2 Oil Palm Fronds as a Biomass Fuel	6
	2.2.1 Gasification of Biomass	6
	2.2.2 Direct Combustion	7
	2.2.3 Characteristics of oil palm fronds	7
	2.3 Drying Principles	8
	2.3.1 Heat transfer	8
	2.3.2 Water removal	10
	2.4 Types of Dryers	10

CHAPTER 3:	METHODOLOGY	16
3.1	Project Flow	16
3.2	Apparatus	19
3.2.1	The Fresnel lens	19
3.2.2	The lens holder	20
3.2.3	Drying chamber	25
3.3	Petioles as Sample	29
3.4	Drying Test	29
CHAPTER 4:	RESULTS AND DISCUSSION	33
4.1	Solar Drying Test Results	33
4.1.1	Results of the 1st sample	33
4.1.2	Results of the 2nd sample	35
4.1.3	Results of the 3rd sample	36
4.1.4	Uncertainty analysis of the results	38
4.2	Oven Drying Test Results	41
4.3	Comparison Between Solar and Oven Drying Tests	42
CHAPTER 5:	CONCLUSIONS AND RECOMMENDATIONS	44
REFERENCES	46

LIST OF FIGURES

Figure 1.1: Comparison of ash content of OPF with other biomass resources	2
Figure 1.2: Comparison of energy content of OPF with other biomass resources	2
Figure 2.1: Comparison between Conventional and Fresnel lenses	4
Figure 2.2: (a) Linear and (b) Circular Fresnel lens	6
Figure 2.3: An oil-palm tree and composition of oil-palm fronds (Zahari, et al., 2003)..	7
Figure 2.4: General overview of natural convection cabinet solar dryer	10
Figure 2.5: Solar lumber kiln (Scanlin, 1998)	11
Figure 2.6: Schematic of the hot water dryer (Zhongjia, et al., 2011)	12
Figure 2.7: Schematic of a solar biomass drier (Prasad et al., 2005)	14
Figure 2.8: Stretched lens array with four lenses and receivers (O'Neill, 2008).....	14
Figure 3.1: Project flow chart	17
Figure 3.2: FYP I Gantt chart	18
Figure 3.3: FYP II Gantt chart.....	19
Figure 3.4: A picture of the Fresnel lens used.....	20
Figure 3.5: Dimensions of the lens carrier	21
Figure 3.6: Dimensions of the arms of the holder at full power.....	22
Figure 3.7: New dimensions of the lens carrier at minimum power	23
Figure 3.8: Side view of the lens holder	23
Figure 3.9: Top view of the lens holder	24
Figure 3.10: Isometric view of the lens holder	24
Figure 3.11: The lens holder with the lens fixed on top	25
Figure 3.12: A schematic of the drying chamber with full dimensions	26
Figure 3.13: Metal receiver	26
Figure 3.14: Position of the concentrated beam at sunrise	27
Figure 3.15: Position of the concentrated beam at sunset	27
Figure 3.16: Picture of the drying chamber	28
Figure 3.17: Air flow inside the drying chamber	29
Figure 3.18: Oil palm frond samples	29
Figure 3.19: Solar rig equipment setting	31
Figure 3.20: Setting of the thermocouple probe	32
Figure 3.21: Universal oven model UNB 400.....	32
Figure 4.1: Variation of moisture content in OPF with time for solar and oven drying	43

LIST OF TABLES

Table 3.1: Fresnel lens specifications.....	20
Table 4.1: Results of drying the 1st sample using concentrated solar power	34
Table 4.2: Results of drying the 2nd sample using concentrated solar power	36
Table 4.3: Results of drying the 3rd sample using concentrated solar power	37
Table 4.4: Uncertainty analysis of the moisture content measurements	39
Table 4.5: Uncertainty analysis of the temperature measurements	39
Table 4.6: Uncertainty analysis of the humidity measurements.....	40
Table 4.7: Uncertainty analysis of the solar insolation measurements	40
Table 4.8: Results of drying the three samples using the electric oven	42

CHAPTER 1

INTRODUCTION

1.1 Background of Study

The public concern on environmental issues, especially on the rapid exhaustion of fossil fuels have imposed a huge influence on people around the world nowadays to find alternative sources of fuels that are environmental friendly. With respect towards this issue, renewable energy has been considered as the primary option of energy sustainability after fossil fuel. The most promising types of renewable energy are biomass. Biomass is defined as an organic matter available on a renewable basis, including forest and mill residues, wood wastes, agricultural crops and wastes, animal wastes and municipal solid waste.

Malaysia is amongst the world's top producers of palm oil with the present planted area is increasing to around 4.0 million hectares. Despite of the huge production, the oil consists of only about 10% of the total biomass produced in the plantation. The other 90% (Empty Fruit Bunch (EFB), trunks, kernels, and palm oil mill effluent) are rejected as waste or left to settle in waste ponds, while Oil Palm Fronds (OPF) are left to rot for soil nutrition (Abdulmuin et al., 2001). An average of 54.43 million tons per year of oil palm fronds was estimated to be available during the replanting process in the years of 2007 – 2020. Abundant research has been carried out by MARDI and JIRCAS on use of OPF for animal feeding, either fresh, or processed as silage or pellet in which four processing methods have to be carried out for OPF, namely pelleting, dry chopping, silage, and Na OH treatment (Zahari et al., 2008).

This project concentrates on oil palm fronds, as they are easier to collect, store and to prepare as feedstock. OPF possess a higher quality in terms of lower ash content, higher calorific value and acceptable moisture content compared to other biomass resources as shown in Figure 1.1. Figure 1.2 shows that the oil-palm fronds (OPF) contain a calorific

value higher than those of other available biomass feeds such as wheat straw, cereal straw, corn stalk, switch grass and vine shoot, but lower compared to conventional fossil fuels such as coal. It was also concluded that the OPF has average density of 712.8 kg/m^3 from a physical property analysis. Thus it is more suitable as compared to other feedstock materials in terms of bulk handling (Abdulmuin et al., 2001).

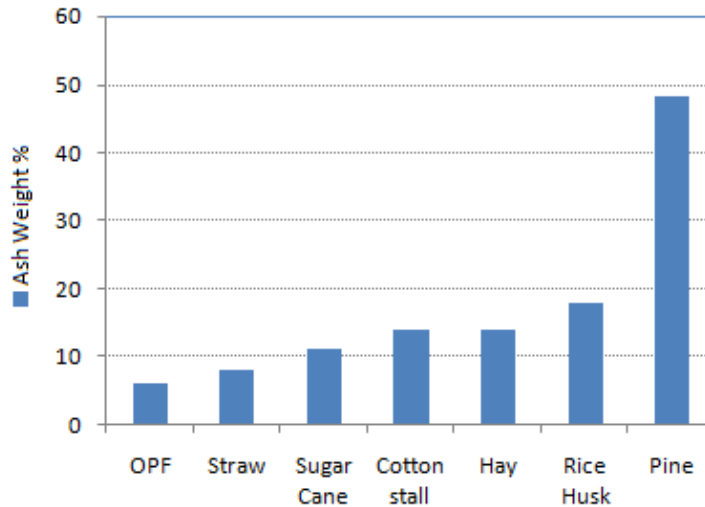


Figure 1. 1: Comparison of ash content of OPF with other biomass resources (Balamohan, 2008)

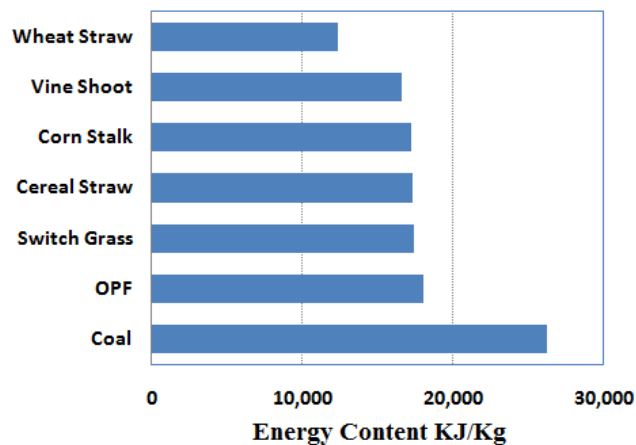


Figure 1.2: Comparison of energy content of OPF with other biomass resources (Balamohan, 2008)

For industrial use it's used in boilers, gasifiers, brick kilns, furnaces, foundries and power plants. It's used as well for residential and Commercial Heating applications. It

produces less smoke and less CO₂ compared to other materials, it has low moisture, dust and impurities content. It's an environment friendly material, and it's easy to transport and store.

1.2 Problem Statement

A challenge of using oil palm frond as a biomass energy source is its high water content which reduces the possibility of ignition in the process and reduces the quantity of product gas due to the need to evaporate the additional moisture before combustion or gasification, compared to dry fuel in which all the heat goes to heating the air and the products of combustion, as a result an increased flame temperature is reached. In addition high water content makes it costly to transport and manage. Costly drying methods such as by using electric heater make the fronds a non-attractive fuel. Traditional drying i.e., open sun drying had taken 11 days for drying the rhizomes while solar biomass drier took only 1.5 days and produced better quality produce (Prasad, et al., 2005). In addition to the considerable losses that occur during this drying process because of influences such as rodents, birds, insects, rain and microorganisms, as a result the fronds might rot after some time. Hence a clean, low cost and efficient method of drying of oil palm fronds is required.

1.3 Objective

The objective of this project is to conduct a preliminary study of drying OPF using solar energy and focusing lenses. An efficient system for drying oil palm fronds that depends on a sustainable and renewable source of energy was designed. The system was tested; in order to confirm achieving the desired output.

1.4 Scope of Study

The scope of this study is to investigate the effectiveness of using Fresnel lenses for achieving higher temperatures out of concentrated solar thermal energy by obtaining experimental data and analyzing the results for drying oil palm fronds. If more time was allocated, another experimental study was to be conducted; in order to study the drying process using exhaust gases out of a diesel engine.

CHAPTER 2

LITERATURE REVIEW

2.1 Refracting Concentrators

By using concentrating collectors; solar energy is optically concentrated before being transformed into heat. Concentration is achieved by refraction of solar radiation making use of the difference of the speed of light in different mediums; acrylic and air. A refraction index of 1.2 means that light travels 1.2 times as fast in vacuum as it does in water. Snell's law governs the refraction. The refracted light is concentrated in a focal zone, thus multiplying the energy flux in the receiving target.

The difference between a conventional lens and a Fresnel lens is illustrated in Figure 2.1. The design allows the creation of a better aperture and a shorter focal length with less mass and volume of material that would be required by a conventional lens. The surface is made up of many small concentric grooves, eliminating the bulk material. Each groove is approximated by a flat surface that reflects the curvature at that position of the conventional lens, so each groove behaves like an individual prism (Sierra and Vázquez, 2005).

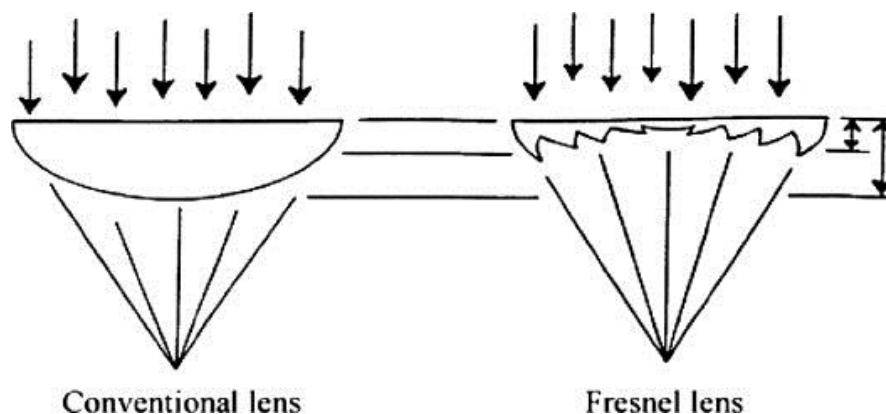


Figure 2.1: Comparison between conventional and Fresnel lenses (Sierra and Vázquez, 2005)

As shown in Figure 2.2, there are two basic Fresnel lens configurations: linear (a) and circular (b). A linear Fresnel lens has linear parallel grooves and the focused light is in the form of a line. A circular Fresnel lens has circular concentric grooves and the focused light is in the form of a circular spot. For the linear lens used in this project the focal zone is a line of width 4 inches (10 cm) at the focal length.

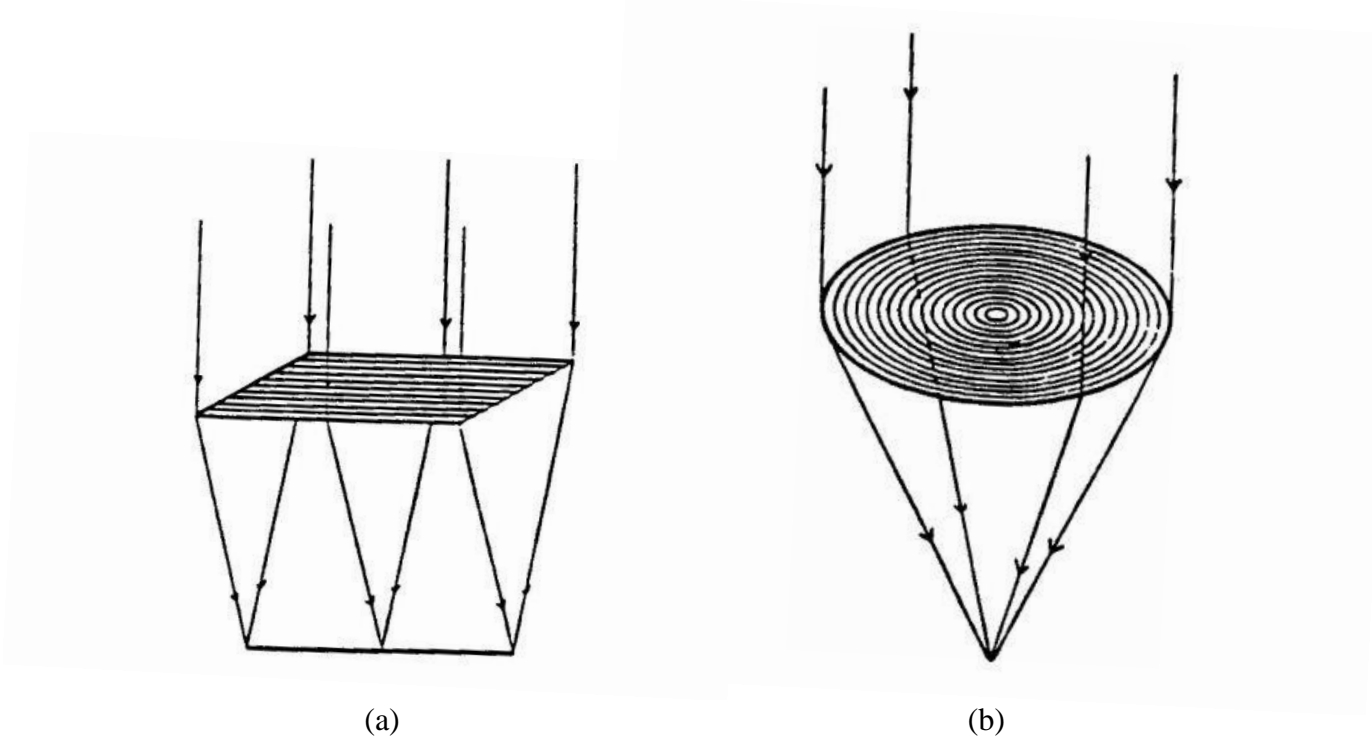


Figure 2.2: (a) Linear and (b) Circular Fresnel lens (Sierra and Vázquez, 2005)

2.2 Oil Palm Fronds as a Biomass Fuel

Oil palm fronds can be converted industrially into a fuel source by two means; gasification and direct combustion.

2.2.1 Gasification of Biomass

Gasification is a process that changes organic or fossil based materials into carbon monoxide, hydrogen, carbon dioxide and methane. This can be accomplished by placing the material at high temperatures without combustion, with a controlled supply of

oxygen. Syngas is the resulting gas mixture, which later is used as the fuel. One of the processes involved in the gasification is the dehydration or the drying process. The biomass is heated at around 100°C for some time until it is totally dry.

2.2.2 Direct Combustion

It's the easiest and cheapest way of utilizing the biomass, yet the least efficient and most hydro carbon-producing. Simply the biomass is burnt in a boiler for generation of high temperature steam in power plant or for other applications e.g. space heating. The first stage in the direct combustion process is the drying of biomass, and it's usually done inside the furnace.

2.2.3 Characteristics of oil palm fronds

An oil palm frond consists of two main components which are petioles and leaflets, as shown in Figure 2.3. Dry matter weight ratio of petiole to leaflets is 1.5 to 1.0. It contains about 18.5% hemicelluloses and moisture contents of fresh leaflets and petioles range from 54-56% and from 75-79% (Zahari et al., 2003). Whether the Oil Palm Fronds will be used in gasifiers or will be directly burnt (direct combustion or co-firing), or will be used as animal feed stocks, the fronds are chopped, and dried to reach a moisture content lower than 30% w.b.

A study by Balamohan (2008) shows that the oil palm fronds with less moisture content are capable of performing well in a gasifier producing syngas with high heating value. This can be compared to the poorer performance of those fuels with moisture content above about 30%. Ignition is made difficult and the quantity of the product gas is reduced; due to the need to evaporate the additional moisture before combustion/gasification can take place (Mckendry, 2001). The moisture content value obtained is lower than other available biomass fuels. Pruned oil-palm fronds are normally left on the ground within the plantation area. Consequently, the oil-palm fronds contain high moisture and it is not suitable to be used directly as a biomass fuel. The high moisture content (higher than 30%) reduces the possibility of ignition in the process and reduces the quantity of product gas due to the energy consumed in order to

evaporate the additional moisture before combustion or gasification processes can start (Balamohan, 2008).

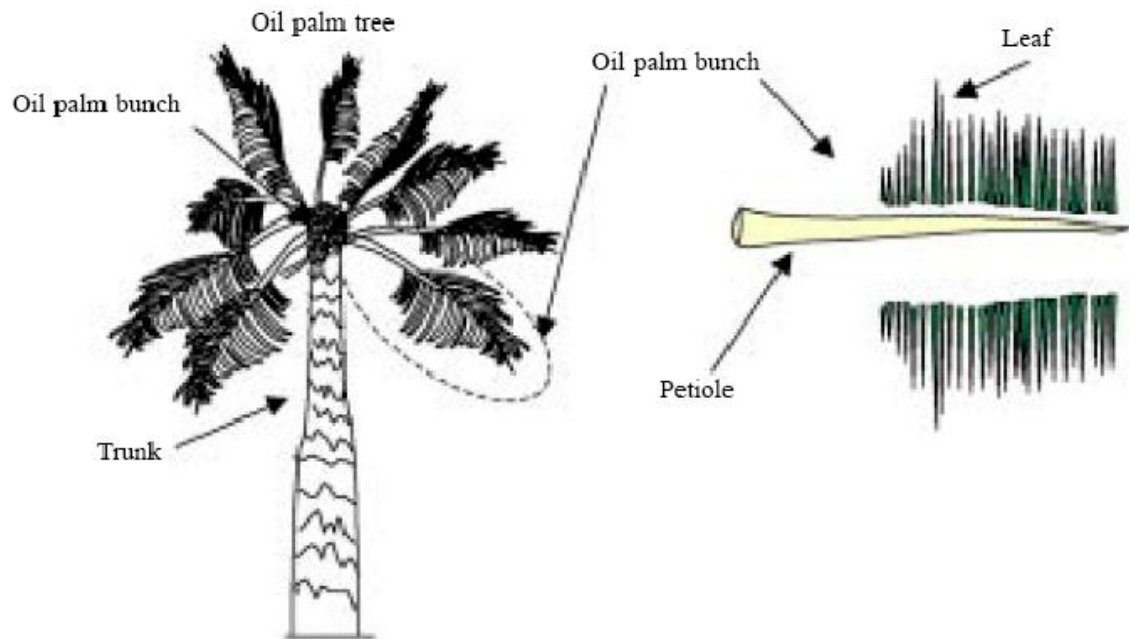


Figure 2.3: An oil-palm tree and composition of oil-palm fronds (Zahari et al., 2003)

2.3 Drying Principles

According to Liptak (1998), there are two requirements for drying which are; the source of heat and method of removing the induced moisture.

2.3.1 Heat transfer

Different forms of heat transfer need to be studied in order to assess the sources of heat just as what happens in the real case.

i. Conduction

It is a mode of transfer of energy within and between bodies of matter, due to a temperature gradient. Heat naturally tends to flow from a body at a higher temperature to a body at a lower temperature. In the absence of external driving forces, temperature differences, over time, approach thermal equilibrium. Equation (2.1) explains this phenomenon. It is known as Fourier's law of heat conduction.

$$Q = - KA \frac{\Delta T}{\Delta x} \quad (2.1)$$

where Q is the magnitude of heat transfer rate, K is the thermal conductivity of the material, A is the area normal to the direction of conduction, and ΔT is the temperature difference, Δx is the distance travelled in the direction of conduction.) (Cengel et al, 2010).

ii. Convection

It is another form of heat transfer from one place to another by the migration of fluids (which is air in this case). When the fluid motion is caused by buoyancy forces that result from the density variations due to deviations of temperature in the fluid, it is known as natural convection. Below is the equation that describes this form:

$$Q = h A (T_s - T_\infty) \quad (2.2)$$

where h is the convection heat transfer coefficient, A is the surface area through which convection heat transfer takes place, T_s is the surface temperature, and T_∞ is the temperature of the fluid sufficiently far from the surface.) (Cengel et al., 2010).

iii. Thermal Radiation

It is the electromagnetic radiation generated by the thermal motion of charged particles in matter. All matter with a temperature greater than absolute zero emits thermal radiation. Sunlight is thermal radiation generated by the hot plasma of the Sun. formula for the Thermal energy transferred can be written as follows:

$$Q = \epsilon \sigma T^4 A \quad (2.3)$$

where q = heat transfer per unit time (W), ϵ = emissivity of the object, $\sigma = 5.6703 \times 10^{-8}$ (W/m²K⁴) - The Stefan-Boltzmann Constant, T = absolute temperature Kelvin (K), A = area of the emitting body (m²). (Cengel et al., 2010).

2.3.2 Water Removal

A study performed by Amos (1998) shows that there are two main stages of drying. For the first stage, heating up the material to wet bulb temperature takes place, in order to force water to leave the wet material. In addition, evaporation of any surface moisture on the material will take place where this process will occur quickly. Then, the material will be heated to drive water from the inside of biomass to the surface to ensure that it can be evaporated. This stage occurs during 'falling rate period'. During this period, surface temperature of material remains close to the wet bulb temperature. Finally, the material begins to heat up the surrounding temperature when the material is completely dry.

There are two occasions in the process of drying when there is a possibility of fire risk. It will occur after the surface moisture has evaporated but before a considerable amount of water has been driven out of the biomass. Another factor is when the material is over dried.

2.4 Types of Dryers

Few of the papers which are concerned with drying different types of biomass using solar energy are reviewed below. Basically one of the following modes of operation presented is utilized. Natural convection is one of these modes in which the air motion is not generated by any external source (like a fan) but only by density differences occurring due to temperature gradients. In natural convection, air surrounding a heat source receives heat, becomes less dense and rises. The surrounding, cooler fluid then moves to replace it. This cooler fluid is then heated and the process continues. The second mode of operation is forced convection in which the air motion is generated by an external driving source. Most of the projects which are presented use solar energy as the source of heat, and some of the projects that employ forced convection use

Photovoltaic cells to power the fans. Another innovative mode of operation is the hybrid design, where solar combined with another source of heat energy are used.

i. Natural Convection Drying

In the design shown in Figure 2.4; solar radiation is transmitted through the single-layered transparent glass at the top and is absorbed by the black colored receiver surface. Insulation is applied to the bottom of the dryer. Thermo Cole is sandwiched between an underside commercial board sheet and an inner side blackened metallic sheet. Owing to the trapped energy, the internal temperature increases. Holes are drilled through the base to allow fresh ventilating air to enter the cabinet. As the temperature increases, hot air rises and leaves from the upper aperture by natural convection, creating a partial vacuum and drawing new fresh air up through the base. Consequently there is a continuous perceptible flow of air over/through the drying material placed on the perforated trays retained in a horizontal position (Sharma et al., 1995).

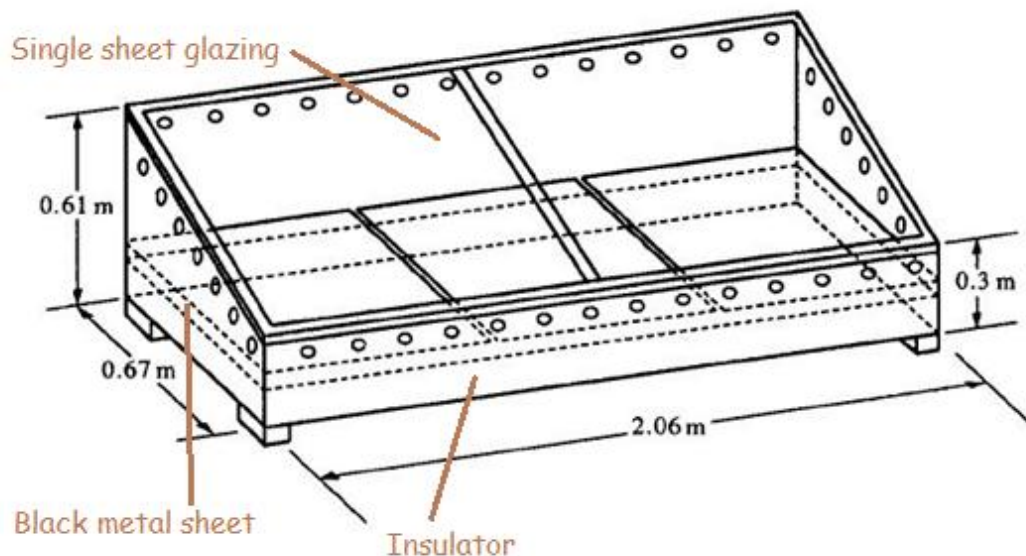


Figure 2.4: General overview of natural convection cabinet solar dryer (Sharma et al., 1995)

ii. Forced Convection Drying

Figure 2.5 shows the design of a low temperature solar thermal collector which is used for lumber drying (wood in any of its stages from felling through readiness for use as structural material for construction). The temperature desired for lumber drying is between 100 and 180° F (the same as for food drying). A solar kiln has the same basic components as most solar thermal technologies: a south facing glazing; glass is a perfect material having as high as 91% solar transmittance and as low as 1% IR transmittance such that it would let a lot of solar energy in but not much heat radiate out. However, it is heavy, and breakable. Another component is the absorbing material; 6 layers of dark gray aluminum window screening to absorb solar energy and convert it to heat. Insulation and tight construction are used in order to reduce unwanted heat loss. There exists an air intake, flow path and exhaust area and an area for lumber pile. Air is drawn into the kiln by three fans, powered by a single Solarex PV module (Scanlin, 1998).

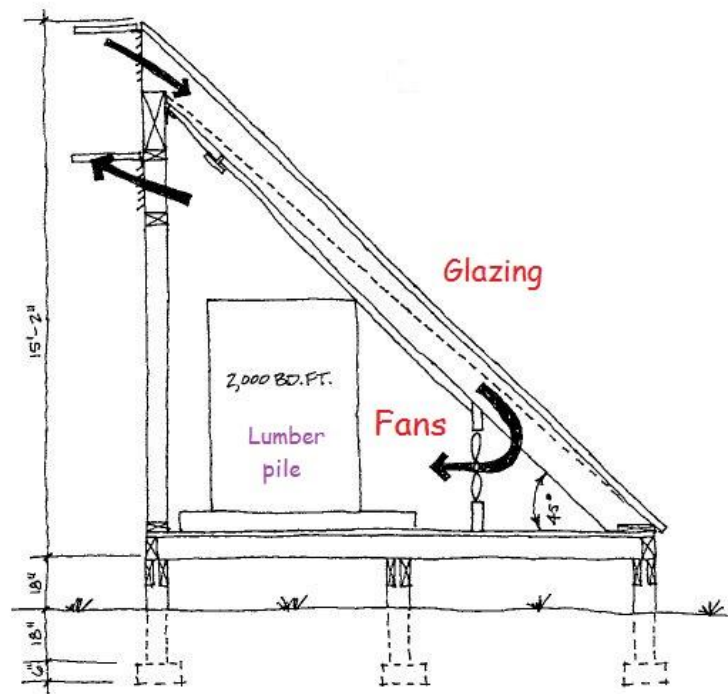


Figure 2.5: Solar lumber kiln (Scanlin, 1998)

Another design for forced convection drying is shown in Figure 2.6; the drier presented in this design consists of a metal mesh belt driven by a pulley that is actuated by a motor. The metal mesh drags the horizontal movement of materials. Circulating fan drives air circulating in the device.

Firstly, the air which is heated through the heat exchanger takes away the moisture from wet materials, and the humid air reenters the circulating fan along the pipe from the bottom outlet. The humid air is exhausted through the air vent and the dry air is made up through air added (Zhongjia et al., 2011).

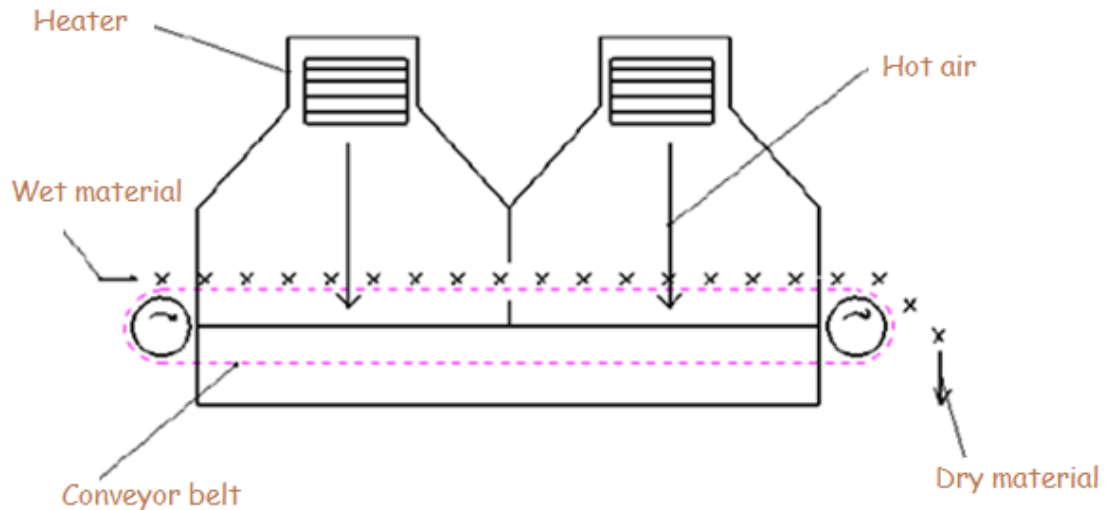


Figure 2.6 Schematic of the hot water dryer (Zhongjia et al., 2011)

iii. Hybrid Drying System

This project presents a direct type natural convection solar drier integrated with a simple biomass burner, using wood as biomass. The design shown in Figure 2.7 makes use of solar energy during day time and biomass during night time as source of heat. The system consists of a single glazed solar cabinet drier fixed on a rock slab. The rock slab is mounted on a chamber made of bricks. The drier has three drying trays of wire mesh base. Three adjustable vents are located at the top of the rear panel of the drier.

The biomass burner contains an adjustable door at the bottom. Its function is for feeding the biomass and controlling airflow for combustion and an iron grate is provided for burning biomass. The exhaust gases exit through a chimney and a flue pipe placed on one side of the biomass burner. A brick chamber encloses this biomass burner. The system is capable of producing a sufficient and continuous flow of hot air temperature between 55 and 60 °C. Turmeric rhizomes were successfully dried using this system. Quantitative analysis used 15 kg of turmeric rhizomes (5 kg on each of the tray) for study. Results showed that it took 36 and 42 h for drying tray 1 and tray 2, respectively whereas in open sun drying it was 266 h for drying of the same product from moisture content of 78% w.b. to 9% w.b. during that trial. Challenges that faced this design is the uniformity of drying as there were significant variations in measured drying parameters at different tray levels during day and night with higher drying efficiency in the upper trays. It was observed that from morning to noon, rhizomes at east side having higher temperature than west side. But from afternoon to the evening the reverse happened. All the time rhizomes at central position had higher temperature than other positioned rhizomes (corners), as air velocity at center was higher compared to other positions (Prasad et al., 2005).

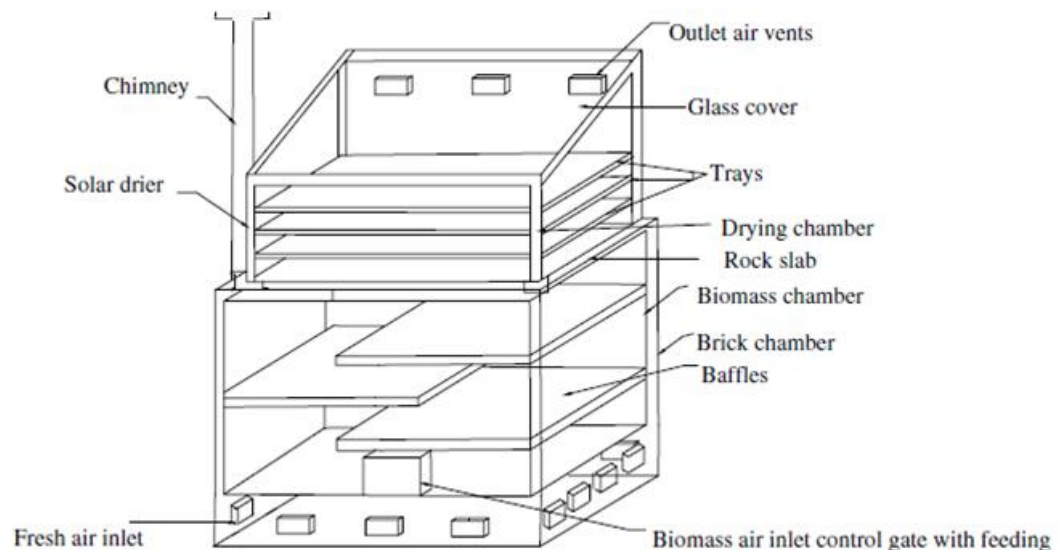


Figure 2.7: Schematic of a solar biomass drier (Prasad et al., 2005)

Since concentrating lenses were implemented for the current design, the following design shown in Figure 2.8 was reviewed. It's utilizing Fresnel lenses for concentration of solar power on photovoltaic cells space power applications. The concentrator encompasses a line-focus Fresnel lens from space-qualified transparent silicone rubber material. The stretched lens is used to collect and focus sunlight at 8 times concentration onto high-efficiency multi-junction photovoltaic cells, which directly convert the incident solar energy to electricity (O'Neill, 2008).

These stretched Fresnel lenses can be implemented in the current design for concentrating the solar rays and accelerate the air heating process since it has a concentration ratio of 8. The lenses act as a shelter for the biomass and protect it from external harmful factors such as bad weather conditions, rain and dust accumulation, and birds such that there wouldn't be a need for other procedures to be taken for protecting the oil palm fronds.

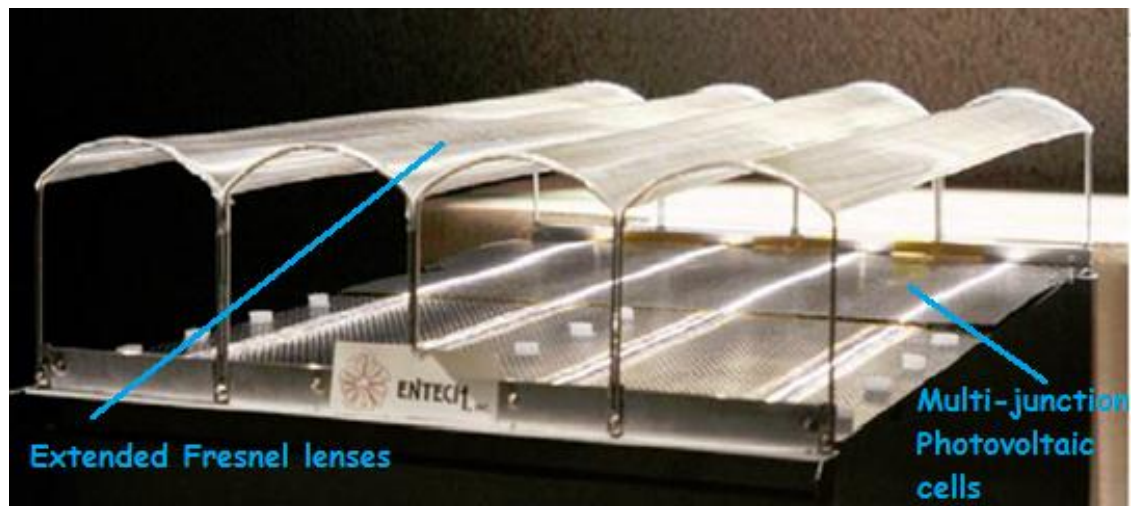


Figure 2.8: Stretched lens array with four lenses and receivers (O'Neill, 2008)

CHAPTER 3

METHODOLOGY

3.1 Project Flow

The project flow is as shown in Figure 3.1. The plan covers both semesters 1 and 2. First, parameters that affect the drying process were studied, such as: temperature, humidity, and air flow. Next a design for the dryer was created fulfilling all the required design parameters. Then all the required materials were purchased for the prototype, the Fresnel lens, the aluminum for the lens holder, and the acrylic for the glazing of the drying chamber. Experiments were done for identifying the time needed for the complete drain of OPF samples, and tracing humidity content versus time, and determining the maximum temperature that could be reached without harming the oil palm frond material. The results were compared with another drying test, which was conducted using an electric oven.

The designing stage took most of the time during the whole project. Drying tests were conducted using many samples, more than one time. The average of the results found was taken in order to have acquired more efficient and more reliable results.

The plan originally was to modify the design in the event that the expected results after running the experiments weren't met. Redesigning of the process was to be performed until the required results were met (e.g. the average temperature of the heated air inside the drying chamber is low compared to what is expected, the solar rig is modified). Major modifications in the original design didn't take place, since the planning stage covered all the possibilities that might happen in the future. Only minor changes and adjustments to the procedures and the steps deviated from the original plan while carrying out the experiments.

A second phase for the project was planned to be combined to the first one if time permits. The second phase was to study the use of exhaust gases out of diesel engines in the drying process.

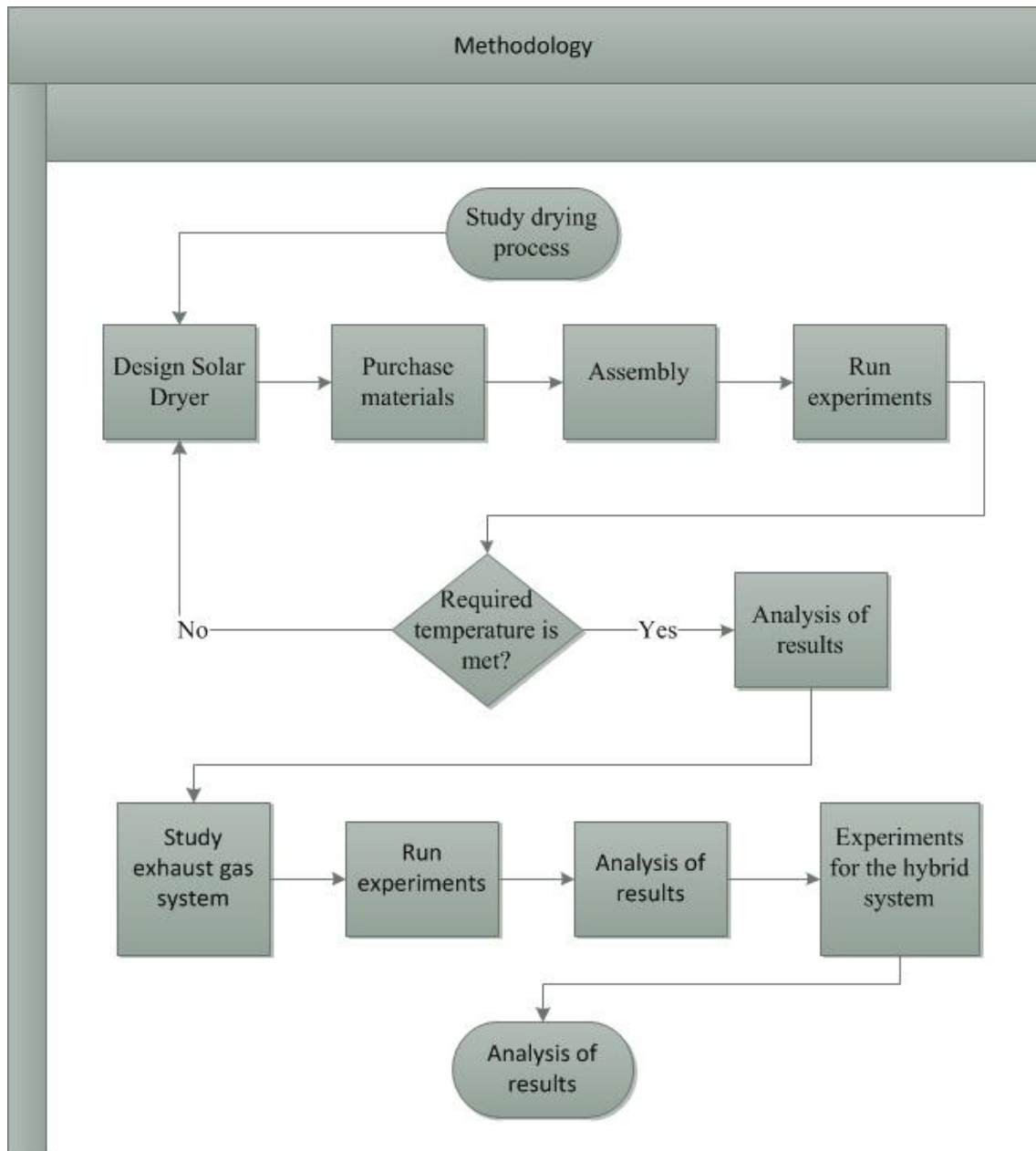


Figure 3.1: Project flow chart

Gantt Charts

The project work started with preliminary research in order to understand the expected outcome of the project work. Literature review extended from the 4th Week until Week number 13 in order to search for any related technical papers, research papers and journals related to solar drying techniques. A secondary research was performed starting from Week 7 until Week 9; its objective was to cover all the aspects of the reviewed projects and to understand their findings. Rig design was planned to be done between Week 11 and Week 12, but due to lack of time during the first semester, designing of the solar rig was moved to the following semester, as shown in Figure 3.2.

Week Number/Task		1	2	3	4	5	6	7	8	9	10	11	12	13	14
Topic selection	P	█													
	A	█													
Preliminary research	P		█	█											
	A		█	█											
Literature review	P				█	█	█	█	█	█	█	█	█	█	
	A				█	█	█	█	█	█	█	█	█	█	
Extended Proposal	P					█	█								
	A					█	█								
Secondary Research	P							█	█	█					
	A							█	█	█	█	█	█	█	█
Proposal Defence	P										█				
	A										█				
Solar rig design	P											█	█		
	A											█	█		
Interim Draft Report	P													█	
	A													█	
Interim Report	P														█
	A														█

Figure 3.2: FYP I Gantt chart

According to the plan; FYP II should start with the solar rig design, where the mode of operation, and the materials used were to be chosen. The Fresnel lens was to be designed and fabricated by the 4th Week. However, some difficulties were met during the fabrication process after consulting several acrylic manufacturing facilities where the required specifications were difficult to be met. An alternative for fabricating the lens was found to be purchasing the lens online. Fresnel lens suppliers were very limited, and were mostly located either in China or the U.S.A. The required size of the lens was found at a supplier's in the U.S.A. By the end of the 6th Week the lens arrived at UTP. Building a holder for the lens and drying chamber that contains the receiver took two whole weeks. The drying tests were performed between Week 9 and Week 10. By Week 12, results were fully collected and their analysis was completed.

Week Number/Task		1	2	3	4	5	6	7	8	9	10	11	12	13	14	15	
Solar rig design	P	█															
	A	█															
Lens purchase	P		█	█	█												
	A		█	█	█	█											
Stand and receiver fabrication	P					█	█										
	A							█	█								
Experimentation (Solar)	P									█	█						
	A																
Results analysis	P											█	█				
	A																
Technical Paper	P														█		
	A																
Oral Presentation	P															█	
	A																
Project Dissertation	P																█
	A																

Figure 3.3: FYP II Gantt chart

3.2 Apparatus

The apparatus which was designed and fabricated for running the experiments consists of three main parts: the Fresnel lens, the lens holder, and the drying chamber where the oil palm fronds will be placed to dry.

3.2.1 The Fresnel lens

The material of the lens shown in Figure 3.4 is acrylic resin (Poly Methyl-Methacrylate, PMMA), which has a long lifetime under the sun light, a good transparency in the solar spectrum, and a low cost of mass production. The refractive index of PMMA is 1.49 which is close to that of glass (Mansour, 2005). The aim was to have a lens with a radius of curvature and a concentration ratio as high as possible, in order to minimize the focal length and thus minimize the size of the solar rig. The Fresnel lens was imported from the U.S.A. The total cost of the lens including the shipment cost was RM650. The specifications of the lens are shown in Table 3.1.



Figure 3.4: A picture of the Fresnel lens used

Table 3.1: Fresnel lens specifications

Focal length	79 cm
Radius of curvature	387.1 mm
Size	99 cm × 73.6 cm
Weight	4.5 kg

3.2.2 The lens holder design

The lens holder is for providing the needed elevation above the ground for the lens. The elevation is measured from the receiver, located inside the drying chamber, to the surface of the lens. The design of the lens holder was chosen to act like a scissor lift; in order to offer the option to adjust the height of the lens from the ground according to the required temperature. The dimensions of the Fresnel lens as shown in Table 3.1 are 990 mm × 736 mm. The dimensions of the lens carrier were made a bit longer than these dimensions in order for the lens to fit in it. These dimensions are shown in Figure 3.5 to be 1015 mm × 745 mm.

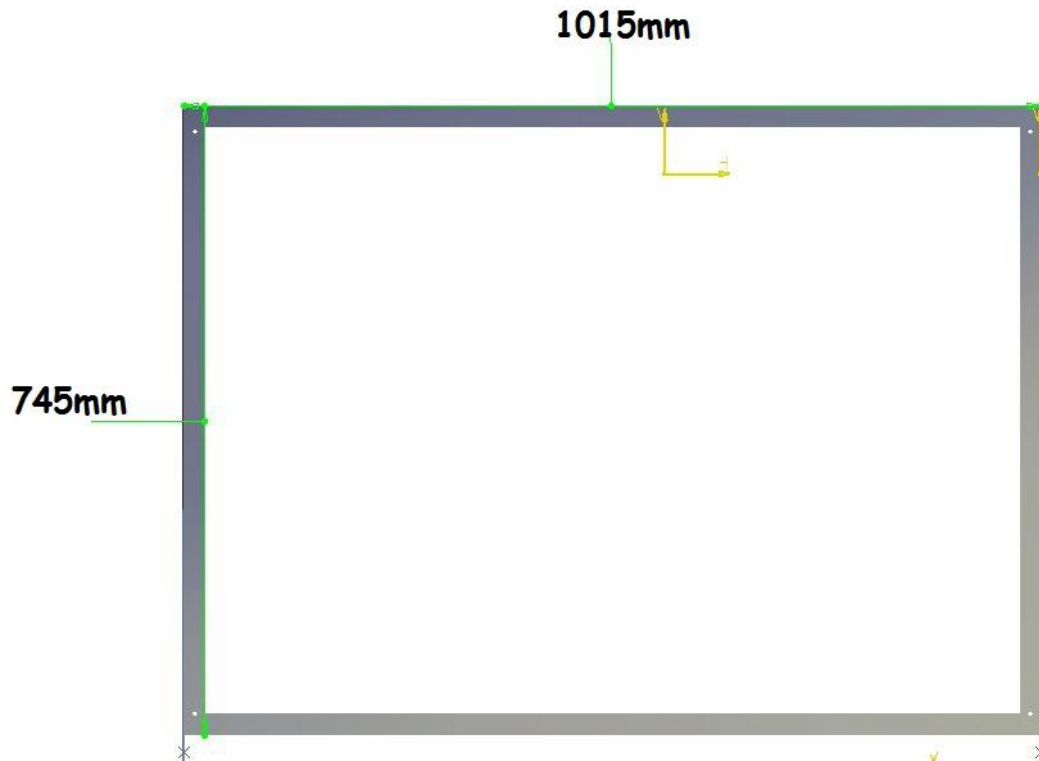


Figure 3.5: Dimensions of the lens carrier

Since the maximum power of concentration or heating could be achieved by adjusting the lens holder to have a distance between the lens and the receiver equals the focal length (790 mm), the length of the arms of the lens holder was chosen to be 1086 mm as shown in Figure 3.6.

For having a beam of a wider surface area; in order to spread the heat more evenly on the surface of the receiver, the elevation of the lens should be shortened. It was found out that for an elevation shorter than 450 mm, the focused light beam began to converge again. Thus a minimum concentration value could be obtained at an elevation of 450 mm. In order to have this elevation without changing the length of the arms of the holder, the lens carrier dimensions needed to be extended. Figure 3.7 shows the new dimensions of the carrier for the new configuration. The new configuration would offer various elevations for the lens, by adjusting the width of the lens carrier with a maximum power at width of 745 mm and a minimum power at a width of 988 mm.

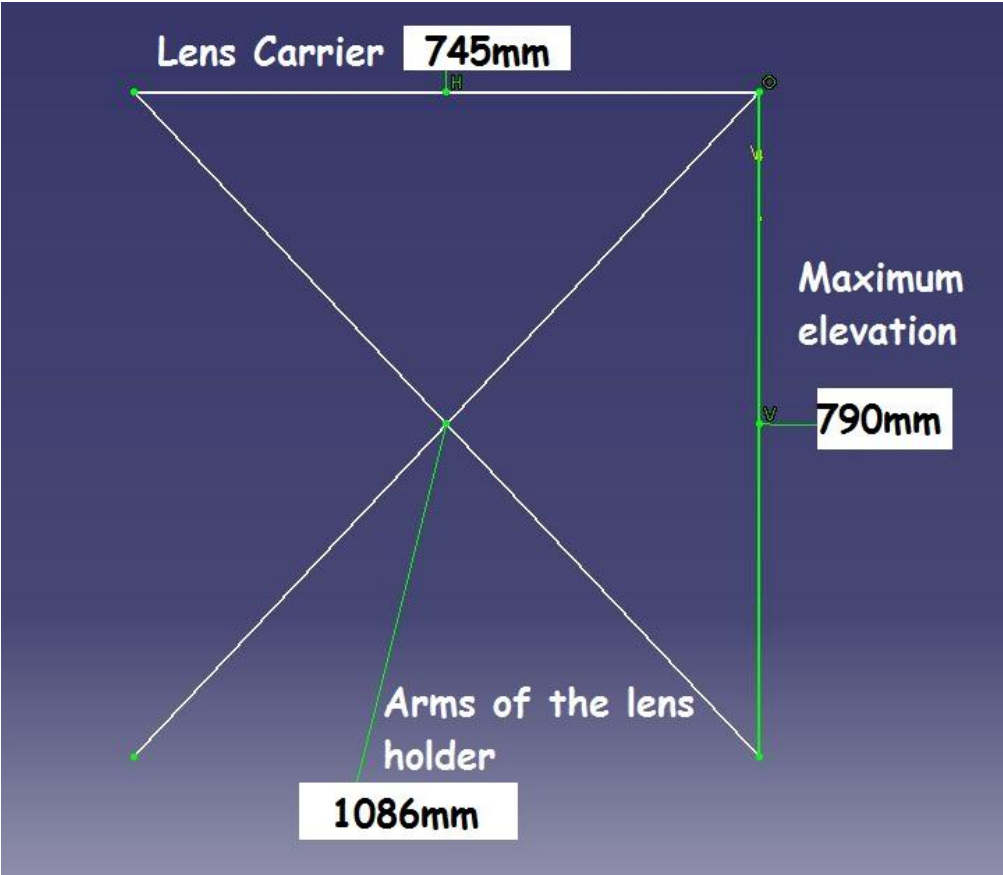


Figure 3.6: Dimensions of the arms of the holder at full power

The lens holder was chosen to be fabricated from aluminum L-plates; since aluminum is light, abundant and has relatively good strength compared to other metals. Experimental analysis has proved that an elevation of 512 mm will limit the temperature inside the drying chamber to a maximum of 110°C, during receiving the maximum solar irradiance (910 W/m² which usually takes place between 12p.m.-2 p.m.); in order not to harm the organic material of the biomass.

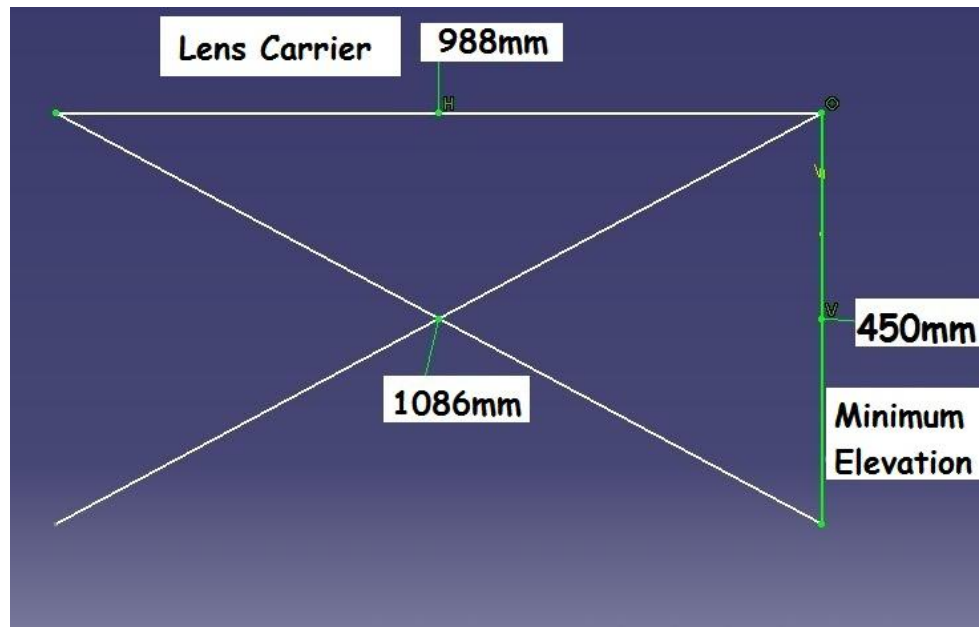


Figure 3.7: New dimensions of the lens carrier at minimum power

Figure 3.8 shows a side-view for the complete design of the lens holder, and Figure 3.9 shows a top-view. Figure 3.10 shows an isometric view for the lens holder adjusted to an elevation of 512 mm. A picture of the lens holder after fabrication with the lens fixed on top is shown in Figure 3.11.

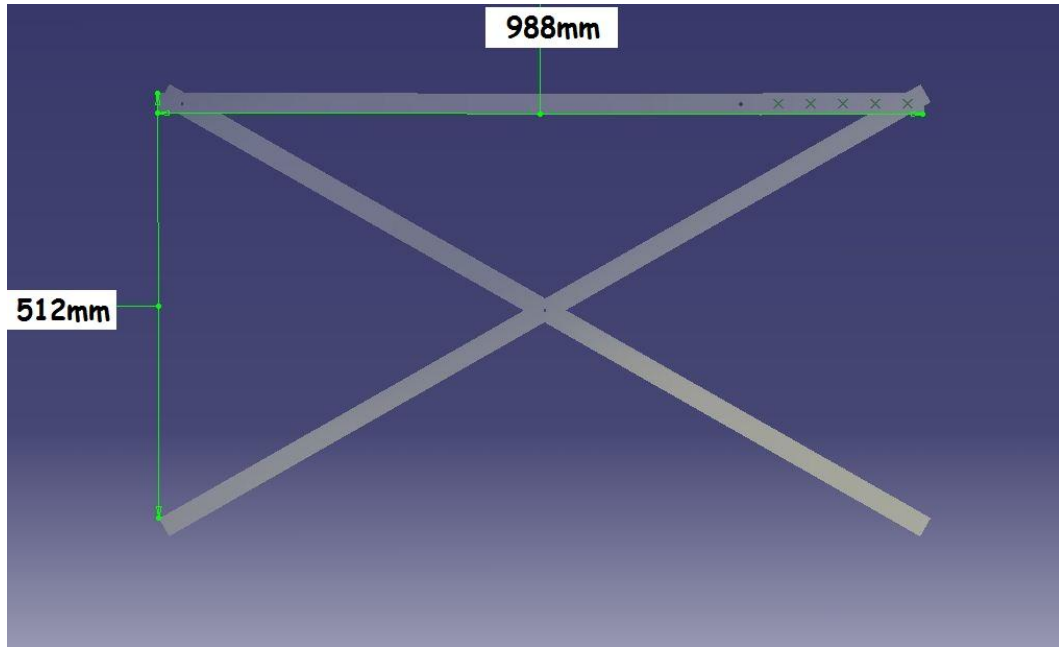


Figure 3.8: Side view of the lens holder

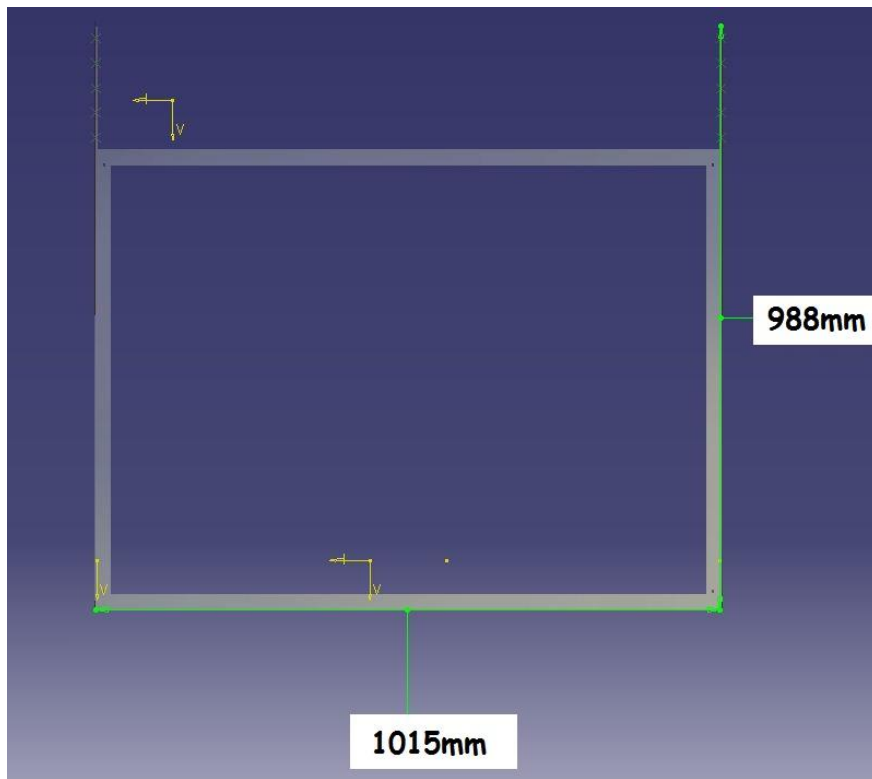


Figure 3.9: Top view of the lens holder

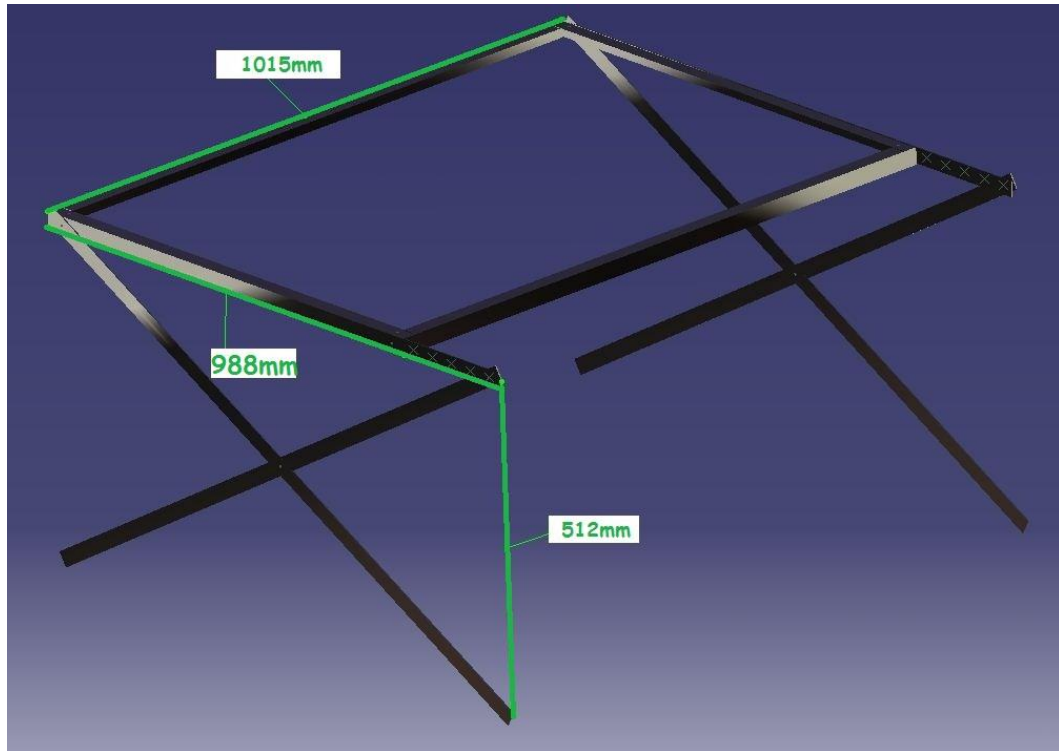


Figure 3.10: Isometric view of the lens holder adjusted to an elevation of 512 mm

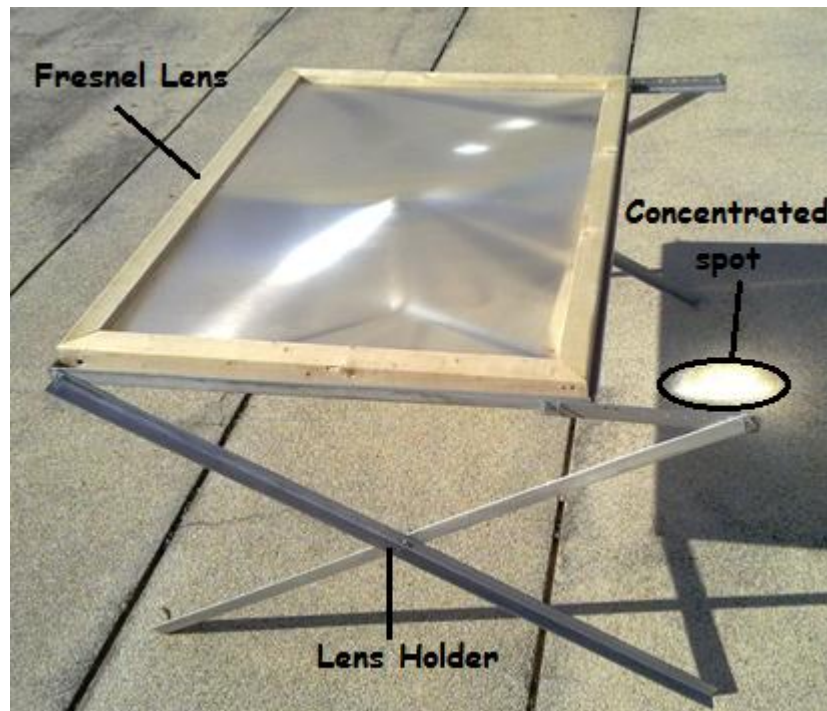


Figure 3.11: The lens holder with the lens fixed on top

3.2.3 Drying Chamber

The receiver is the part of the apparatus designed to absorb the radiant energy out of the lens, and conduct the heat energy into the surrounding air until satisfying temperature is reached. The chamber consists of two parts; the receiver and the glazing. Figure 3.12 shows a schematic of the drying chamber. Its dimensions are 910 mm × 210 mm. The two holes at each side of the glazing are highlighted as well in the picture.

The receiver is a piece of metal made of aluminum of thickness 3 mm. aluminum has high thermal conductivity (250 W/m.K) which makes it a perfect choice for a uniform distribution of the heat through the whole length of the drying chamber and for a faster heat transfer by conduction to the air inside the chamber.

The receiver is elevated from the ground surface in order to enhance conduction of the heat from the metal sheet to the air inside the drying chamber; through both the bottom and top surfaces of the absorber. As shown in Figure 3.13; it's painted in black in order to enhance the absorptivity of the solar radiation and minimize its reflectivity. The dimensions of the receiver were set in order for the black surface to contain the focused light beam at different times of the day. This eliminates the need for a sun tracking mechanism, and hence minimizes the capital and maintenance costs of the solar dryer.

The aluminum sheet is designed to receive light from the sun at different times of the day starting from sun rise until sunset. The orientation of the lens is as shown in Figure 3.14, where the lens will be positioned parallel to the East-West line. Since the sun is moving from east to west during the day time, the beam of the concentrated light will move accordingly from west to east. Figures 3.14 and Figure 3.15 show the positions of the concentrated beam of light at sunrise and sunset.

The second part of the drying chamber is the transparent cover. Its function is simply to trap the hot air inside the chamber from escaping and trap the reflected solar rays from the plate thus raising the temperature inside the chamber in a shorter time. All the sides of the cover will be made from 12 mm sheets of acrylic as shown in Figure 3.16.

Acrylic is chosen since it has a thermal conductivity of 0.2 W/m.K , which is very low, in order to act as an insulator and minimize the heat transfer from the hot air inside the chamber into the atmospheric air through conduction and/or convection.

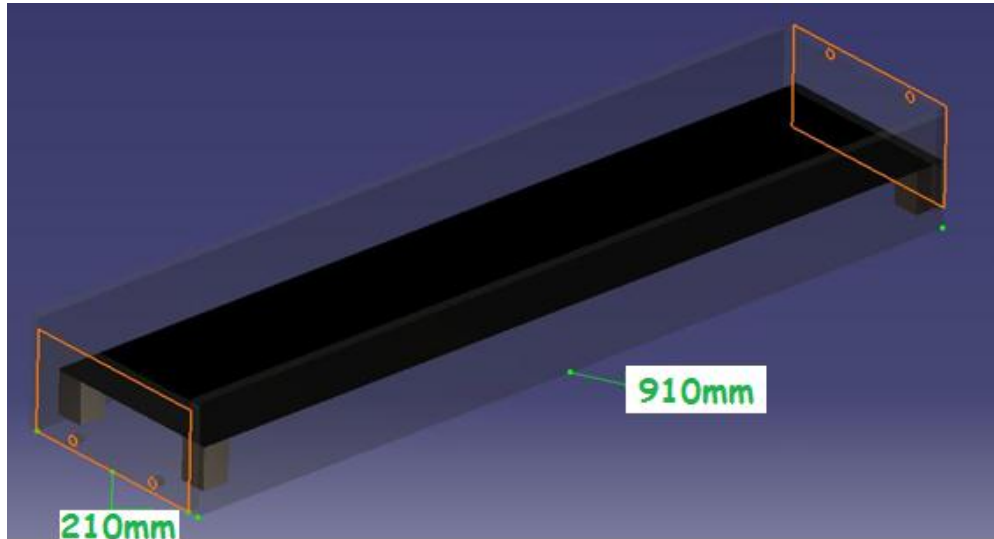


Figure 3.12: A schematic of the drying chamber with full dimensions

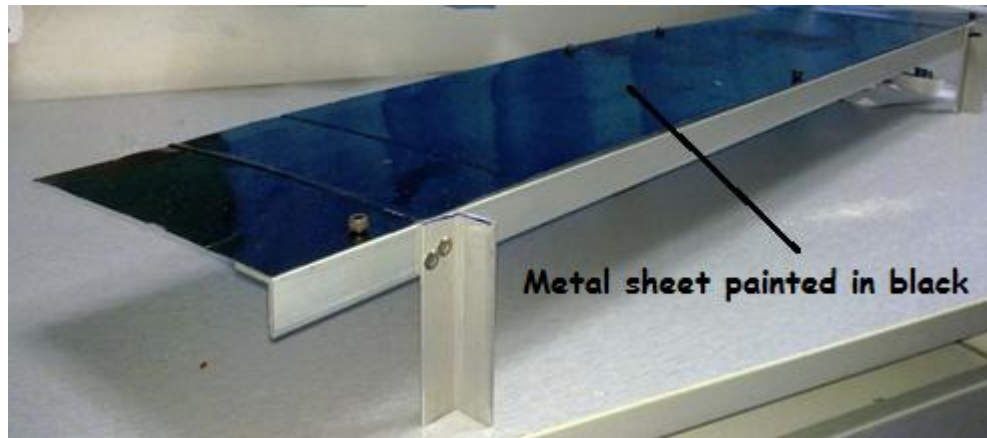


Figure 3.13: Metal receiver

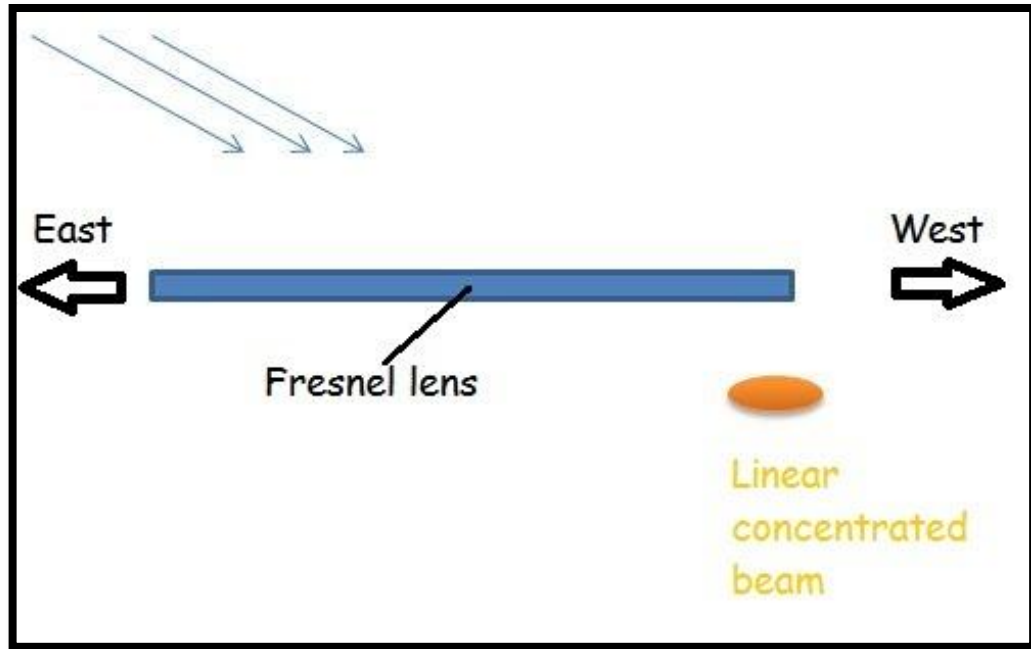


Figure 3.14: Position of the concentrated beam at sunrise

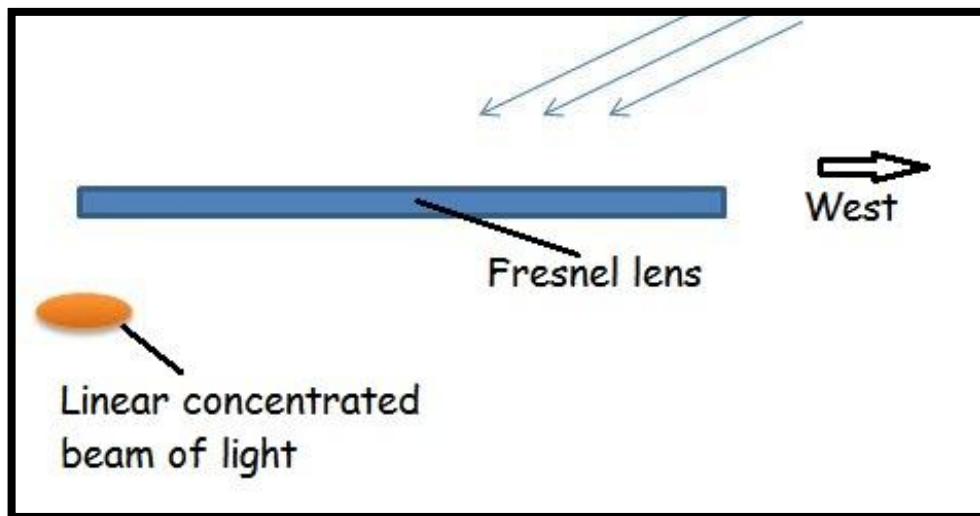


Figure 3.15: Position of the concentrated beam at sunset

The top surface of the cover was designed to be made from a sheet of glass of thickness 5 mm. This thickness is chosen in order to minimize the reflection and the absorbance of the solar radiation passing through the cover. As shown in Figure 3.17 two holes

were made at the bottom right side of the glazing acting as fresh air inlet and another two holes at the top left side of the cover acting as moist air outlet. These holes were made to induce some ventilation inside the chamber; in order to get rid of the relative humidity inside the chamber, thus accelerating the drying process. Figure 3.17 shows the airflow inside the drying chamber as well. As the collected beam heats the metal sheet (receiver), the air surrounding the biomass is heated and rises up by natural convection (illustrated by the yellow arrow in the figure). The moisture removed from the biomass will be carried upwards during the rising action of the hot air. Then the moist air will leave the drying chamber through the hole located on the upper left side of the chamber, causing a drop in the pressure. This drives fresh air from outside to enter the chamber and thus maintaining the relative humidity inside the chamber at a lower level.

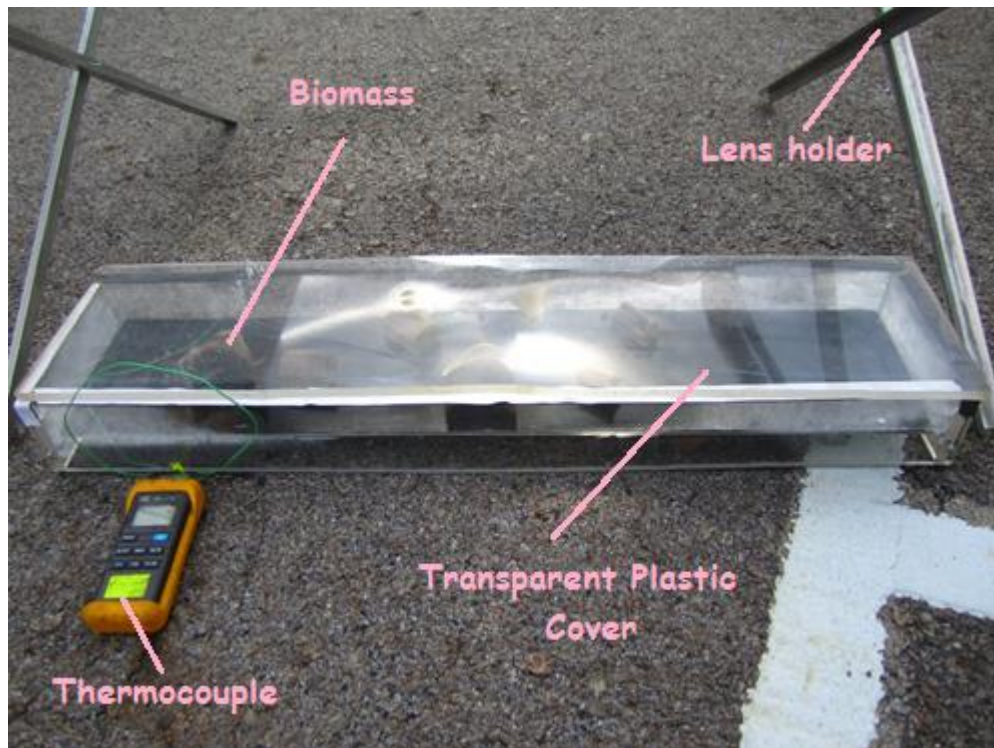


Figure 3.16: Picture of the drying chamber

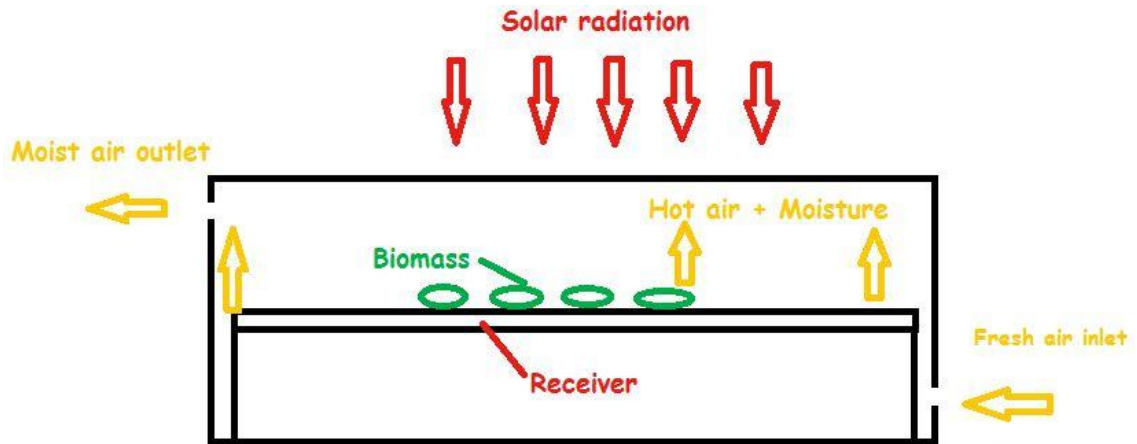


Figure 3.17: Air flow inside the drying chamber

3.3 Petioles as sample

The oil palm frond samples shown in Figure 3.18 were freshly pruned at the oil-palm plantation in Kampung Bali, Tronoh. All leaflets were shredded away using cleaver to obtain only a petiole as a main sample to be investigated. Petioles were cut into small pieces such that the length of each sample is nearly 3 cm.

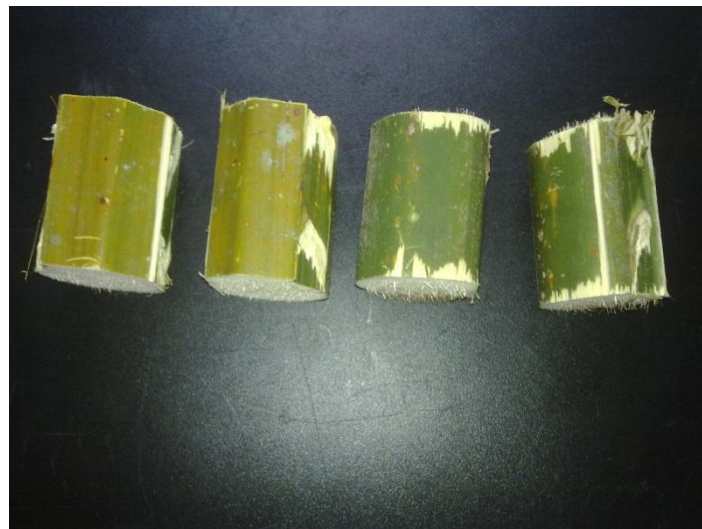


Figure 3.18: Oil palm frond samples

3.4 Drying Test

Drying tests were performed using the solar rig in order to know the drying rate of the biomass. To compare the results of the proposed technique with the existing drying techniques, another type of drying tests were performed using an electric oven.

The first one was performed using the new prototype, depending on concentrating solar thermal power as the source of heat. Setting of the equipment is shown in Figure 3.19. Before running the experiment, each piece was marked with a unique mark and its original weight was recorded in order to keep track of the moisture content. Weight measurements were taken using Ohaus TS4KD Precision Standard Top-Loading Balance with an accuracy of ± 0.02 g. For each half an hour, each sample's weight was recorded in order to determine the percentages of moisture loss from the sample. To calculate the percentage of moisture loss from each sample, the following equation was used:

$$X\% = ((W_0 - W) / W_0) \times 100 \quad (3.1)$$

where X is the percentage of moisture loss, W_0 is initial mass of the sample, and W is the mass of the sample after drying. Solar insolation was recorded using a Solarimeter. When not much difference in the sample's weight existed, the samples were placed in the oven at a temperature of 105 degrees and the difference in weight is kept track of on an hourly basis until there's not any change in the weight. This is to make sure the samples were completely moisture free.

Humidity measurements were recorded using Extech 407412A Heavy Duty Hot Wire Hygro-Thermo-Anemometer with an accuracy of $\pm 3\%$. Temperature measurements were taken using an RS thermocouple of type K, with an accuracy of $\pm 2.5^\circ\text{C}$. Measurements were taken on an hourly basis at various points inside the drying chamber. The solar drying tests were approximately conducted at the same time of the day. The tests started at 10.0 a.m. and ended at 5.0 p.m. The thermocouple used for measuring the temperature was installed at the receiver's surface. To make sure that the

actual air temperature inside the chamber was measured, the thermocouple was always placed away from the solar radiation as shown in Figure 3.20.

The second drying test was performed using an electric oven. The oven used for this experiment is Universal Oven Model UNB 400, as shown in Figure 3.21. The oven has natural convection application and continuous adjustment of pre-heated fresh air admixture. The oven is installed with microprocessor PID-temperature controller assisted by integrated auto diagnostic system with fault indicator. In order to control the temperature. Same procedures and steps like the first test were repeated.

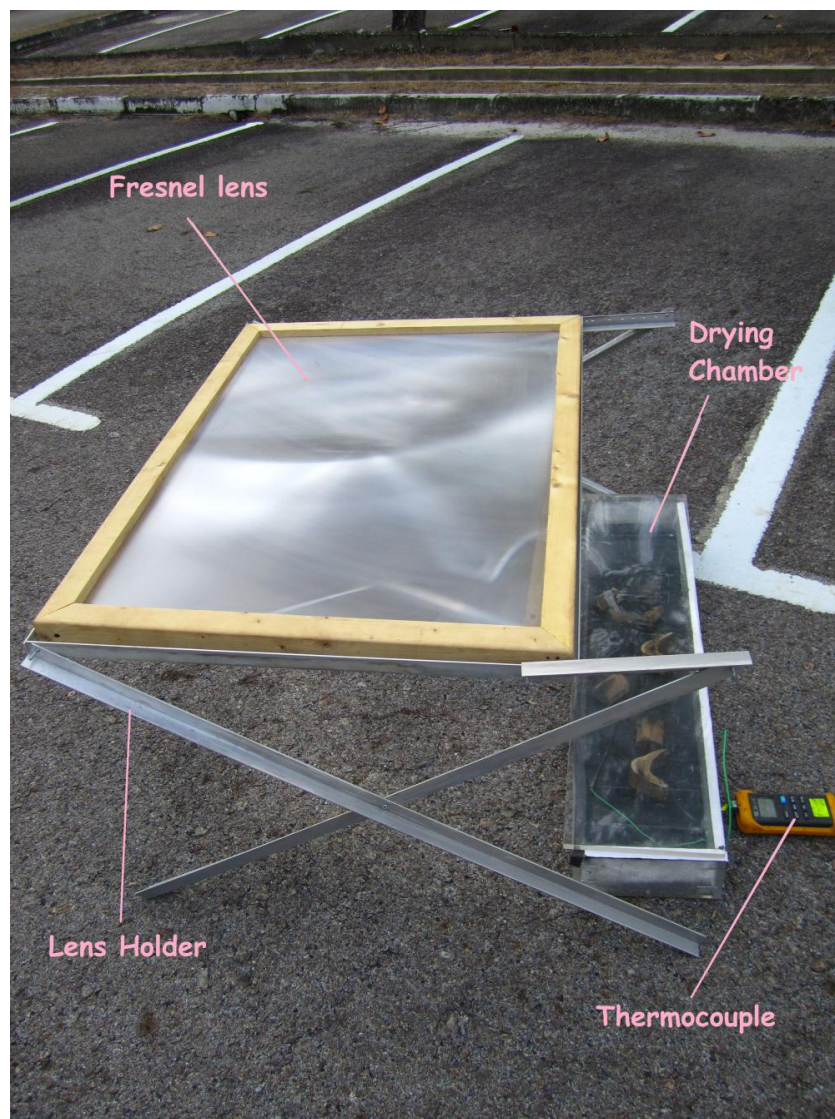


Figure 3.19: Solar rig equipment setting

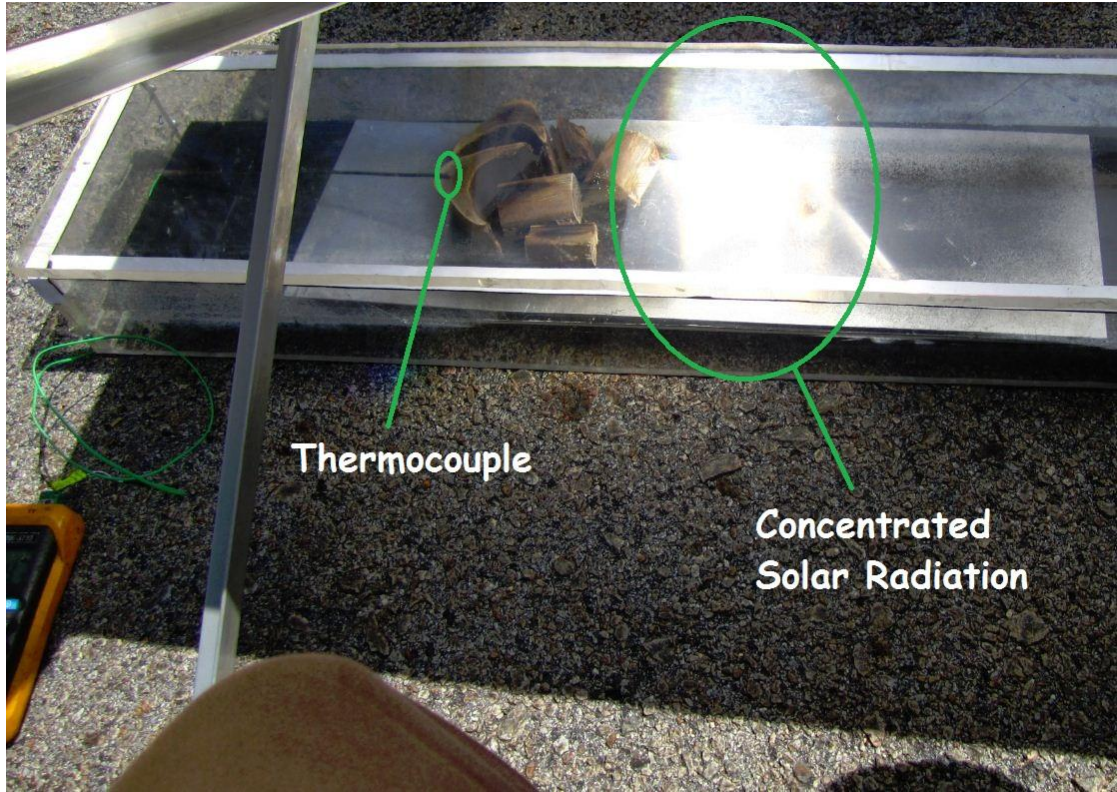


Figure 3.20: Setting of the thermocouple probe



Figure 3.21: Universal oven model UNB 400

RESULTS AND DISCUSSION

4.1 Solar Drying Test Results

Drying tests were performed on the samples on different days; from the morning until the evening. Those days were chosen when the sky was nearly as clear from clouds as possible. Random samples were chosen on different days of running the tests.

5.1 Results of the 1st sample

Results of drying the first sample are shown in Table 4.1. After drying the first sample for 7 hours, it was found out that there was not weight loss taking place anymore. Total moisture content of the biomass sample was 38.41grams, which is 57.07% of the original weight of the sample. It was dried from a moisture content of 57.07% w.b. to 0% w.b. The average temperature during the drying process inside the drying chamber was 99.46°C, with a maximum value of 110°C and a minimum value of 88°C. This depended heavily on the weather conditions and whether the sky is cloudy or not; since radiation is the most effective heat transfer mechanism for this test. As stated in the designing stage of the lens holder, a distance of 512 mm between the lens and the drying chamber will limit the temperature inside the chamber to a maximum of 110°C; in order not to harm the organic material of the biomass.

The relative humidity inside the chamber depended heavily on the relative humidity of the air outside the chamber, this is due to the continuous airflow; bringing fresh air from outside the chamber. Inside the chamber the humidity value always exceeded the humidity value of the atmospheric air. However, the difference wasn't big (around 3%).

The average irradiance received from the sun for this day was 611.92 W/m² which is considered to be high. It reached a maximum value of 907 W/m² and a minimum value of 340 W/m². All solar insolation measurements were taken directly under the sun. The average drying rate for this sample was 5.49 g/hr.

Table 4.1: Results of drying the 1st sample using concentrated solar power

Duration (hour)	Weight	Moisture Removal	Inside Drying Chamber		Outside condition		Solar Insolation (W/m ²)
			T _i (°C)	ϕ _i (%)	T _o (°C)	ϕ _o (%)	
0.0	67.30	0.00	30.0	82	30.0	82	500
0.5	56.00	16.79	110.0	86	31.0	83	759
1.0	38.50	42.79	109.0	86	32.0	84	826
2.0	35.20	47.70	105.0	86	32.0	84	826
2.5	34.70	48.44	90.0	83	28.0	81	400
3.5	31.00	53.94	93.5	81	34.0	79	600
4.0	29.50	56.17	91.0	73	33.0	70	586
4.5	29.48	56.20	88.0	70	31.0	68	340
5.0	29.01	56.89	110.0	52	35.6	50	907
5.5	28.97	56.95	100.0	69	35.0	65	400
6.0	28.94	57.00	95.0	63	32.4	62	560
6.5	28.89	57.07	96.0	49	32.0	48	601
7.0	28.89	57.07	95.0	49	32.0	48	650
Total Weight Loss (g)	38.41						
Average Drying Rate (g/hr)	5.49						

To find the system efficiency, equation 4.1 is used.

$$\eta\% = (P_{\text{drying}}/P_{\text{in}}) \times 100 \quad (4.1)$$

where P_{in} (W) is the solar incident power, and P_{drying} (W) is the drying power. Equation 4.1 is used to calculate the incident power (Cengel et al, 2010).

$$P_{\text{in}} = Ee \times A \times \eta \quad (4.2)$$

where Ee is the radiant flux density (W/m²), A (m²) is the area of the Fresnel lens, η is the efficiency of the Fresnel lens that accounts for reflected and absorbed radiation by the lens. It was assumed to be 50%. To calculate the drying power, both sensible and latent energy need to be included. To calculate the sensible heat energy used for drying equation 4.3 is used (Cengel et al, 2010).

$$Q_{\text{sensible}} = m \times C_p \times \Delta T \quad (4.3)$$

Where m is the mass (g) of water removed, and C_p is the specific heat capacity of liquid water at constant pressure (4.1813 J/g.K) and ΔT (K) is the change in temperature.

Latent heat of vaporization of water was calculated to be 86.69 kJ. Sensible heat energy was calculated using equation 4.3 to be 12.05 kJ. The total drying energy for one sample is the sum of both sensible and latent energies which is found to be 98.74 kJ. By assuming that all the conditions will be the same for all the other samples when the system is at full capacity (30 samples), the total drying energy will be 2962.2 kJ. By dividing with the duration of drying (6.5 h), the drying power was found to be 126.6 W. With an average irradiance of 611.92 W/m², the solar incident power was calculated using equation 4.2 to be 223.25 W. Thus, the system's efficiency was calculated using equation 4.1 to be 56.7%.

4.1.1 Results of the 2nd sample

Drying test results for the second sample are shown in Table 4.2. After drying the first sample for 6 hours, it was found out that there was not weight loss taking place anymore. Total moisture content of the biomass sample was 40.8 grams, which is 61.19% of the original weight of the sample. The sample was dried from a moisture content of 61.19% w.b. to 0% w.b. The average temperature during the drying process inside the drying chamber was 99.63°C, with a maximum value of 110°C and a minimum value of 87°C.

A similar trend of the relative humidity progression inside the drying chamber took place as in the 1st drying test. Inside the chamber the humidity value always exceeded the humidity value of the atmospheric air. The average irradiance received from the sun for this day was 695 W/m²; which is higher than the value of the 1st test. It reached a maximum value of 907 W/m² and a minimum value of 340 W/m². The average drying rate for this sample was 5.83 g/hr.

For removing 40.8 grams of water, the latent energy of vaporization of water was calculated to be 92.08 kJ. Sensible heat energy was calculated using equation 4.3 to be 12.8 kJ. The total drying energy for one sample is the sum of both sensible and latent energies which is found to be 104.88 kJ. By assuming that the conditions will be the

same for all the other samples when the system is at full capacity (30 samples), the total drying energy will be 3146.4 kJ. By dividing with the duration of drying (6.5 h), the drying power was found to be 134.5 W. With an average irradiance of 695 W/m², the solar incident power was calculated using equation 4.2 to be 253.68 W. Thus, the system's efficiency was calculated using equation 4.1 to be 53%.

Table 4.2: Results of drying the 2nd sample using concentrated solar power

Duration (hour)	Weight (g)	Moisture Removal (wt%)	Inside Drying Chamber		Outside condition		Solar Insolation (W/m ²)
			T _i (°C)	Ø _i (%)	T _o (°C)	Ø _o (%)	
0.0	70.6	0.00	30.0	86	32.0	83	700
0.5	60.6	19.64	108.0	85	30.0	82	759
1.0	45.3	51.19	108.0	87	31.0	84	726
2.0	41.2	57.14	110.0	83	32.0	80	901
2.5	39.8	57.53	96.0	81	28.0	79	600
3.5	36.7	60.71	93.5	77	34.0	75	596
4.0	34.8	60.71	91.0	73	32.0	70	586
4.5	33.6	60.71	87.0	70	31.0	68.4	340
5.0	31	61.01	108	62	34.0	60	907
5.5	30.6	61.01	110.0	60	35.0	57	810
6.0	29.8	61.04	96.0	60	32.3	58	760
6.5	29.8	61.19	95.0	55	31.0	52	700
7.0	29.8	61.19	93.0	52	31.0	50	650
Total Weight Loss (g)	40.8						
Average Drying Rate (g/hr)	5.83						

4.1.2 Results of the 3rd sample

Drying test results for the third sample are shown in Table 4.3. After drying the first sample for 6.5 hours, it was found out that there was no more weight loss taking place. Total moisture content of the biomass sample was 20.56 grams, which is 57.8% of the original weight of the sample. The sample was dried from a moisture content of 57.8% w.b. to 0% w.b. The average temperature during the drying process inside the drying chamber was 98.9°C, with a maximum value of 110°C and a minimum value of 91°C. A similar trend of the relative humidity progression inside the drying chamber takes place as in the first and second drying tests. Inside the chamber the humidity value always exceeded the humidity value of the atmospheric air.

The average irradiance received from the sun for this day was 660 W/m^2 which is higher than the value of the first test but lower than the value of the second. It reached a maximum value of 907 W/m^2 and a minimum value of 360 W/m^2 . The average drying rate for this sample was 2.94 g/hr .

Table 4.3: Results of drying the 3rd sample using concentrated solar power

Duration (hour)	Weight (g)	Moisture Removal (wt%)	Inside Drying Chamber		Outside condition		Solar Insolation (W/m^2)
			T_i ($^{\circ}\text{C}$)	ϕ_i (%)	To ($^{\circ}\text{C}$)	ϕ_o (%)	
0.0	33.6	0.00			29.0	60	600
0.5	27	14.16	100.0	66	30.0	63	800
1.0	16.4	35.84	107.0	66	31.0	64	827
2.0	14.4	41.64	105.0	64	31.0	62	800
2.5	14.27	43.63	92.0	63	32.0	60	600
3.5	13.2	48.02	92.0	65	30.0	62	600
4.0	13.2	50.71	91.0	65	30.0	61	600
4.5	13.2	52.41	110.0	62	34.0	59	900
5.0	13.1	56.09	110.0	59	35.6	58	907
5.5	13.1	56.66	100.0	57.5	35.0	56	600
6.0	13.09	57.79	94.0	57.5	33.0	56	560
6.5	13.04	57.79	94.0	57.5	33.0	57	370
7.0	13.04	57.79	92.0	59	32.0	58	360
Total Weight Loss (g)	20.56						
Average Drying Rate (g/hr)	2.94						

For removing 20.56 grams of water, the latent energy of vaporization of water was calculated to be 46.5 kJ. Sensible heat energy was calculated using equation 4.3 to be 6.45 kJ. The total drying energy for one sample is the sum of both sensible and latent energies which is found to be 52.95 kJ. By assuming that all the conditions will be the same for all the other samples when the system is at full capacity (60 samples as this sample was taken from the tip of the OPF; hence it's smaller in size), the total drying

energy will be 3177 kJ. By dividing with the duration of drying (6.5 h), the drying power was found to be 135.8 W. With an average irradiance of 660 W/m², the solar incident power was calculated using equation 4.2 to be 240.9 W. Thus, the system's efficiency was calculated using equation 4.1 to be 56.4%.

The average drying time for the three samples was six and half hours. All the samples were completely dried. The average total moisture content of the three samples was 58.7% of the original weight. The average drying temperature of the three tests was 99.33°C. The average drying rate for the three samples was 4.75 g/hr. The average calculated efficiency achieved for the solar system was estimated to be 55.4%.

The losses can be due to the radiation losses at the cover of the drying chamber, since a thick sheet of acrylic was used. One more factor is the reflective losses at the receiver. Heat losses through conduction and convection can be a major contributor to this low efficiency; due to the openings made in the drying chamber for the purpose of inducing ventilation and removal of humidity inside the chamber. One last factor is the losses induced while taking weight and humidity measurements inside the drying chamber each half an hour. The biggest challenge faced the proposed system was its heavy dependence on solar radiation, which depended heavily on the weather conditions, and the time of the day. Cloudy conditions formed an obstacle for this system

4.1.3 Uncertainty Analysis of the results

The sum squared deviation method was used to estimate the accuracy of all the results. Table 4.4 shows that the calculated error for the weight loss estimated of sample 1, sample 2 and sample 3 due to the moisture removal is 1.97%, 11.23% and 10% respectively.

Table 4.5 shows that the calculated error for the temperature measurements inside the drying chamber for test 1, test 2 and test 3 is 2.82°C, 3.44°C and 5°C respectively.

Table 4.4: Uncertainty analysis of the moisture content measurements

Sample 1	Sample 2	Sample 3	Average	Error 1	Error 2	Error 3
16.79	19.64	14.16	16.87	0.00	0.03	0.03
42.79	51.19	35.84	43.27	0.00	0.03	0.03
47.70	57.14	41.64	48.83	0.00	0.03	0.02
48.44	57.53	43.63	49.87	0.00	0.02	0.02
53.94	60.71	48.02	54.22	0.00	0.01	0.01
56.17	60.71	50.71	55.86	0.00	0.01	0.01
56.20	60.71	52.41	56.44	0.00	0.01	0.01
56.89	61.01	56.09	58.00	0.00	0.00	0.00
56.95	61.01	56.66	58.21	0.00	0.00	0.00
57.00	61.04	57.79	58.61	0.00	0.00	0.00
57.07	61.19	57.79	58.68	0.00	0.00	0.00
57.07	61.19	57.79	58.68	0.00	0.00	0.00
RSS				0.00	0.15	0.12
MRSS				0.00	0.01	0.01
Mean Error				1.97	11.23	10.07

Table 4.5: Uncertainty analysis of the temperature measurements

Test 1	Test 2	Test 3	Average	Error 1	Error 2	Error 3
110.0	108.0	100.0	106.0	0.00	0.00	0.00
109.0	108.0	107.0	108.0	0.00	0.00	0.00
105.0	110.0	105.0	106.6	0.00	0.00	0.00
90.0	96.0	92.0	92.6	0.00	0.00	0.00
93.5	93.5	92.0	93.0	0.00	0.00	0.00
91.0	91.0	91.0	91.0	0.00	0.00	0.00
88.0	87.0	110.0	95.0	0.01	0.01	0.02
110.0	108.0	110.0	109.3	0.00	0.00	0.00
100.0	110.0	100.0	103.3	0.00	0.00	0.00
95.0	96.0	94.0	95.0	0.00	0.00	0.00
96.0	95.0	94.0	95.0	0.00	0.00	0.00
95.0	93.0	92.0	93.3	0.00	0.00	0.00
RSS				0.01	0.01	0.03
MRSS				0.00	0.00	0.00
Mean Error				2.82	3.44	5.01

Table 4.6 shows that the calculated error for the humidity measurements inside the drying chamber for test 1, test 2 and test 3 is 8.44%, 5.46% and 11.83% respectively.

Table 4.6: Uncertainty analysis of the humidity measurements

Test 1	Test 2	Test 3	Average	Error 1	Error 2	Error 3
86	85	66	79	0.01	0.01	0.03
86	87	66	79	0.01	0.01	0.03
86	83	64	77	0.01	0.00	0.03
83	81	63	75	0.01	0.00	0.03
81	77	65	74	0.01	0.00	0.02
73	73	65	70	0.00	0.00	0.01
70	70	62	67	0.00	0.00	0.01
52	62	59	57	0.01	0.01	0.00
69	60	57	62	0.01	0.00	0.01
63	60	57	60	0.00	0.00	0.00
49	55	57	53	0.01	0.00	0.00
49	52	59	53	0.01	0.00	0.01
RSS				0.09	0.04	0.17
MRSS				0.01	0.00	0.01
Mean Error				8.44	5.46	11.83

Table 4.7: Uncertainty analysis of the solar insolation measurements

Test 1	Test 2	Test 3	Average	Error 1	Error 2	Error 3
500	700	600	600	0.03	0.03	0.00
759	759	800	772	0.00	0.00	0.00
826	726	827	793	0.00	0.01	0.00
826	901	800	842	0.00	0.00	0.00
400	600	600	533	0.06	0.02	0.02
600	596	600	598	0.00	0.00	0.00
586	586	600	590	0.00	0.00	0.00
340	340	900	526	0.13	0.13	0.50
907	907	907	907	0.00	0.00	0.00
400	810	600	603	0.11	0.12	0.00
560	760	560	626	0.01	0.05	0.01
601	700	370	557	0.01	0.07	0.11
650	650	360	553	0.03	0.03	0.12
RSS				0.38	0.44	0.77
MRSS				0.03	0.03	0.06
Mean Error				17.10	18.41	24.34

Table 4.7 shows that the calculated error for the solar insolation measurements directly under the sun for test 1, test 2 and test 3 is 17.1 W/m², 18.41 W/m² and 24.34 W/m² respectively.

4.2 Oven Drying Test Results

One drying test was performed on three oil palm frond samples. The drying temperature was set to 105°C. Weight measurements were taken for each sample every half an hour. The results for the three samples are shown in Table 4.8.

Table 4.8: Results of drying three samples using the electric oven

Duration (hr)/ Sample no.	Weight (g)			Moisture Removal (Weight %)			Average (Weight %)	Standard Deviation (weight %)
	Sample 1	Sample 2	Sample 3	Sample 1	Sample 2	Sample 3		
0.0	51.16	49.80	83.70	0.00	0.00	0.00	0.00	0.00
0.5	47.07	45.50	78.56	7.99	8.63	6.14	7.59	1.30
1.0	43.85	42.01	73.44	14.29	15.64	12.26	14.06	1.70
1.5	40.84	39.08	69.74	20.17	21.53	16.68	19.46	2.50
2.0	38.38	36.69	66.32	24.98	26.33	20.76	24.02	2.90
2.5	36.00	34.29	62.80	29.63	31.14	24.97	28.58	3.22
3.0	33.88	32.33	59.64	33.78	35.08	28.75	32.53	3.35
3.5	31.95	30.67	57.01	37.55	38.41	31.89	35.95	3.54
4.0	30.27	29.24	54.44	40.83	41.29	34.96	39.03	3.53
4.5	28.66	27.78	51.59	43.98	44.22	38.36	42.19	3.31
5.0	27.18	26.51	48.62	46.87	46.77	41.91	45.18	2.83
5.5	26.20	25.64	46.66	48.79	48.51	44.25	47.19	2.54
6.0	25.22	24.74	44.66	50.70	50.32	46.64	49.22	2.24
6.5	24.36	23.95	42.63	52.38	51.91	49.07	51.12	1.79
7.0	23.60	23.33	40.64	53.87	53.15	51.45	52.82	1.25
7.5	23.06	22.86	38.98	54.93	54.10	53.43	54.15	0.75
8.0	22.55	22.44	37.26	55.92	54.94	55.48	55.45	0.49
8.5	22.20	22.20	35.92	56.61	55.42	57.08	56.37	0.86
9.0	21.98	22.03	34.77	57.04	55.76	58.46	57.09	1.35
9.5	21.86	21.92	33.74	57.27	55.98	59.69	57.65	1.88
10.0	21.80	21.86	32.82	57.39	56.10	60.79	58.09	2.42
10.5	21.70	21.77	31.83	57.58	56.29	61.98	58.62	2.98
11.0	21.70	21.77	31.83	57.58	56.29	61.98	58.61	2.98
weight loss (g)	29.46	28.03	51.87				36.45	
Average Drying rate (g/hr)	2.81	2.67	3.03				2.84	

4.3 Comparison Between Solar and Oven Drying Test Results

Figure 4.1 combines the results of both of the tests in one plot. The results of three samples from each test can be examined. It's shown in the figure that the time for the complete removal of moisture from the three samples of oil palm fronds (solar 1, solar 2, and solar 3) using the proposed solar system that utilizes concentrated solar power is 6.5 hours. It's also shown that the total time taken for drying three samples of oil palm fronds (oven 1, oven 2, and oven 3) using the electric oven is 10 hours. Moisture content removed in both experiments is approximately 60% of the original weight. The errors for the oven drying test are shown on the graph as well.

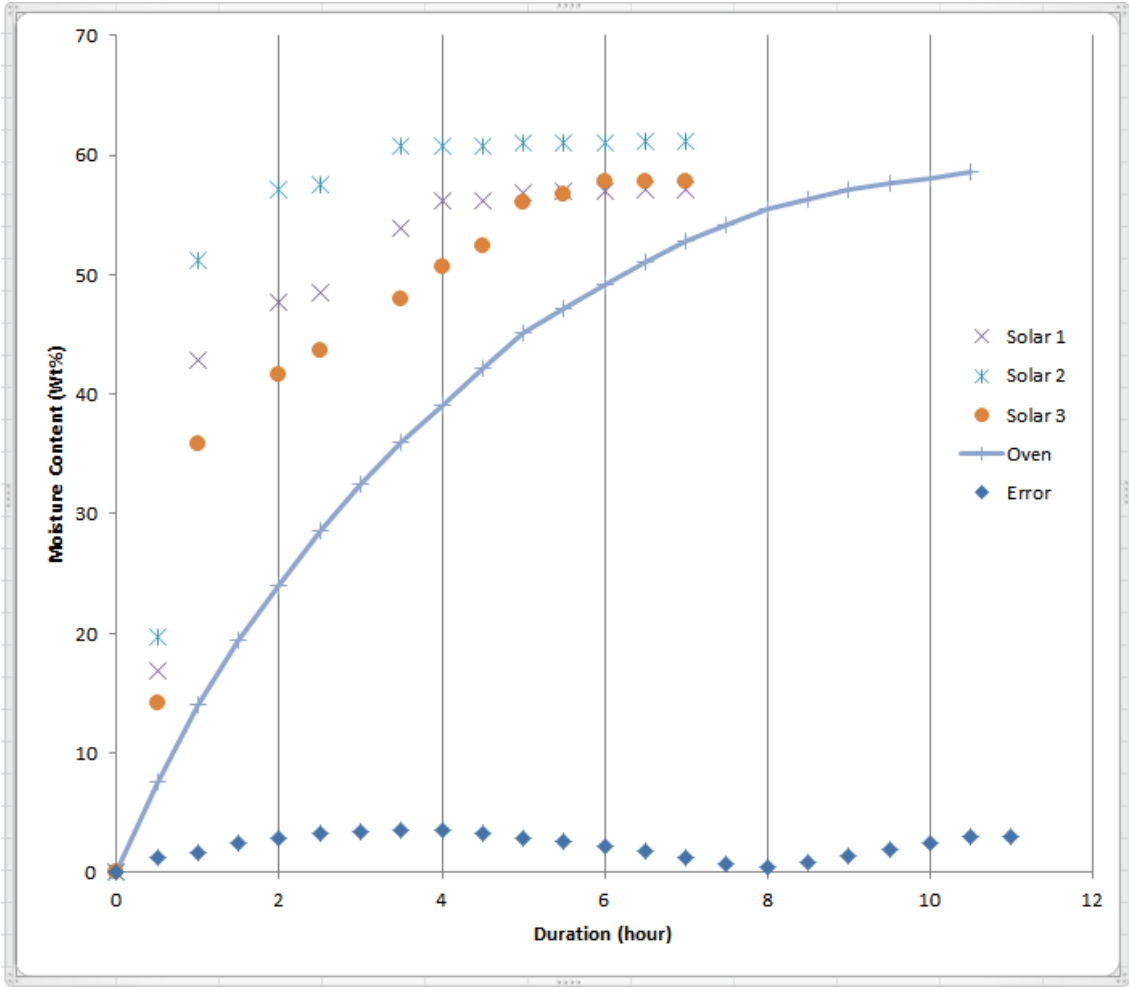


Figure 4.1: Variation of moisture content in OPF with time for solar and oven drying

CHAPTER 5

CONCLUSIONS & RECOMMENDATIONS

The speed of the drying process is affected by several factors which are; the thickness and density of the biomass material, the relative humidity and temperature of the surrounding air, and the speed of the air flow. In general the higher the temperature and air flow are and the lower the humidity is inside the drying chamber; the faster is the drying process. A good solar absorber is dark in color, thin, and has good thermal conductivity. The drying process using solar energy uses the three modes of thermal energy transfer; conduction, convection and radiation. Having all these information, a cheap, efficient and clean solar drying system was created. The system uses a 49 inch Fresnel lens for concentrating the solar radiation on a dark colored metal absorber. A lens holder offers the correct elevation for the lens above the receiver, thus limiting the temperature inside the drying chamber to a 110°C. Glazing is used for trapping the heat energy and trapping the reflected long wave-solar radiation. Glazing is made of a thick insulating material for minimizing the loss of heat energy by conduction and convection. Promising results were obtained using the proposed system compared to current existing systems. Oil palm frond samples were completely dried using concentrated solar thermal energy in 6.5 hours. The average drying temperature of the conducted tests was 99.33°C. The average drying rate for the samples was 4.75 g/hr. Drying using the oven at the same temperature took 10.5 hours, with an average drying rate of 2.81 g/hr. Better results were achieved by the proposed system due to lowering the relative humidity value inside the drying chamber compared to that inside the oven as a result of the better air flow inside the drying chamber. The average efficiency achieved for the three tests using the solar system was estimated to be 55.4%. This was due to the thermal losses that took place while running the tests.

More experiments are recommended to be performed in the future to obtain more consistent results. It was observed that the temperature inside the drying chamber was

non-uniform throughout the area of the receiver, with higher values close to the concentrated light beam. It's recommended to study the temperature values at different areas of the drying chamber, during different times of the day. It's recommended as well to create a map, tracing the accurate motion of the concentrated light beam throughout different times of the day. One more important step to put in mind is to confirm that the oil palm frond samples are totally free of moisture after running the solar drying tests. This could have been done by placing the samples in the electric oven after running the solar drying tests and tracing the change in the weight measurements until there are no more changes in the weight. Since the design depends heavily on the solar intensity, it's recommended to combine a backup heating source to this system, in the event of unstable and cloudy weather conditions. By converting the proposed system into a hybrid one the problem of inconsistent solar radiation will be solved.

CHAPTER 6

REFERENCES

Abdulmuin, M. Z., Alamsyah, T. M. I., & Mukhlisien, D. (2001). An alternative energy source from palm wastes industry for Malaysia and Indonesia, *Energy Conversion and Management Volume 42*, 2109-2118.

Mansour, A.F. (2005). Optical Properties of Fullerene/PMMA. *International Journal of Polymeric Materials*, pp. 227–235.

Amos, W.A. (1998). Report on Biomass Drying Technology, National Renewable Energy Laboratory, U.S Department of Energy.

Atnaw, S. M., & Sulaiman, S. A. (2009). Modeling and simulation study of downdraft gasifier using oil-palm fronds. *Energy and Environment, 2009. ICEE 2009. 3rd International Conference*, 284-289.

Balamohan, S. (2008). Studies on suitability of oil-palm fronds (OPF) for biomass gas production. Department of Mechanical Engineering, Universiti Teknologi PETRONAS, Final Year Project (FYP).

Cengel, Y. A., Ghajar A. J. (2010). Heat and mass transfer, 4th Edition, 27-29.

Hassan, A., Yacob, S. (2002). Utilization of Biomass in Malaysia, Faculty of Biotechnology, Universiti Putra Malaysia.

Liptak, B. (1998). Optimizing Dryer Performance Through Better Control, *Chemical Engineering*; Vol. 105, No. 2, pp. 110-114.

McKendry, P. (2001). Energy production from biomass (part 3): Gasification technologies. *Bio resource Technology*, 83(1), 55-63.

O'Neill, M. J. (2003). Ultralight stretched Fresnel lens solar concentrator for space power applications. *Proceedings of SPIE*, 5179(5179), 116-126.

Prasad, J., Vijay, V. K., Tiwari, G. N., & Sorayan, V. P. S. (2006). Study on performance evaluation of hybrid drier for turmeric (*curcuma longa* L.) drying at village scale. *Journal of Food Engineering*, 75(4), 497-502.

Scanlin, D. (1997). Indirect, Through-Pass, solar food dryer. *Home Power*, 62-72.

Scanlin, D. (1998). The solar lumber kiln. *Home Power*, 50-57.

Sharma, V. K., Colangelo, A., & Spagna, G. (1995). Experimental investigation of different solar dryers suitable for fruit and vegetable drying. *Renewable Energy*, 6(4), 413-424.

Sierra C. and Vázquez, A.J. (2005). High solar energy concentration with a Fresnel lens. *Journal of Materials Science*, pp. 1339–1343.

Zahari, M. W., Oshio, S., Jaafar, D. M., Najib, M.A., Yunus, I. M., & Nor Ismail, M.S. (2008). Voluntary intake and digestibility of treated oil palm fronds. Retrieved

July/2011, from

http://www.jpvpk.gov.my/index.php?option=com_content&view=article&id=253%3Aoil-palm-fronds&catid=36%3Apasture&lang=en.

Zhongjia, C., Xiaohu, L., & Xiangyue, Y. (2011). The research and design of bio-fuel raw material drying system based on high-temperature hot water as the medium. *Power and Energy Engineering Conference (APPEEC), 2011 Asia-Pacific*, 1-4.